Abstract

Title of Dissertation:	A MONTE CARLO AUGMENTED BAYESIAN NETWORK APPROACH TO DEVELOPING HYBRID EXTERNAL FLOOD PROBABILISTIC RISK ASSESSMENTS
	Joy Shuan Shen, Doctor of Philosophy, 2025
Dissertation directed by:	Associate Professor Michelle Bensi, Department of Civil and Environmental Engineering, and Professor Mohammad Modarres, Department of Mechanical Engineering

Nuclear power plant (NPP) sites are potentially vulnerable to external flooding, which can impact the safe operation and shutdown of reactors. Flood protection features mitigate flood risks by preventing floodwater from infiltrating areas housing safety-related systems, structures, and components (SSCs). Flood-related operating experience has highlighted the frequency and severity of external flood impacts on NPP sites. The current state of practice of analyzing external flood risks is predominantly deterministic. However, there is a growing interest in developing a probabilistic risk assessment (PRA) approach to complement the deterministic method to better capture more complex risks, such as external floods.

The U.S. nuclear industry employs PRAs to analyze risks by modeling risks to a plant's operation and ability to safely shut down. In external flood PRA applications, there are three elements: (1) probabilistic flood hazard assessment, (2) flood fragility evaluation, and (3) plant response. This

framework is structured around event trees (ETs) and fault trees (FTs). These tools have supported PRAs for decades. However, the assumptions in the binary state, static treatment of time, and spatial dependencies provide challenges in PRA modeling that are highlighted in external flood applications. Additionally, computational abilities and PRA methods have improved. These tool assumptions and improvements prompted a questionnaire to the international PRA community to understand the needs and trends of performing PRAs and supporting analyses. Given this motivation, there is a research need to explore hybrid external flood PRA frameworks to leverage extensive knowledge in ETs and FTs while strategically integrating tools better suited for external flood modeling.

This dissertation leverages the inherent characteristics of a Bayesian network (BN) to address the limiting assumptions in external flood risk modeling and incorporates questionnaire insights. To mitigate the computational and memory demands that come with BNs, a Monte Carlo simulation integrates out relevant nodes through physical relationships. A hybrid framework then strategically integrates the BN to complement the ETs and FTs. Multiple configurations in which the BN is interfaced with the ETs and FTs are investigated to understand the advantages and limitations of delegating portions of the model to either the BN or ETs/FTs.

A MONTE CARLO AUGMENTED BAYESIAN NETWORK APPROACH TO DEVELOPING HYBRID EXTERNAL FLOOD PROBABILISTIC RISK ASSESSMENTS

by

Joy Shuan Shen

Dissertation submitted to the Faculty of the Graduate School of the
University of Maryland, College Park, in partial fulfillment
of the requirements for the degree of
Doctor of Philosophy
2025

Advisory Committee:
Associate Professor Michelle T. Bensi (Chair)
Professor Mohammad Modarres (Co-Chair)
Professor Katrina M. Groth
Professor Gregory B. Baecher
Dr. Nathan Siu
Professor Mohamad Al-Sheikly (Dean's Representative)

UNIVERSITY OF MARYLAND

11/4/2025

Re: Previously Published Materials appearing in Thesis or Dissertation

Dean of the Graduate School,

Joy Shen (UID:113484650) has:

☐ NOT INCLUDED any previously published works within their thesis or dissertation.

☑ INCLUDED one or more previously published works within their thesis or dissertation. This letter certifies that the examining committee for the student has determined that the student made a substantial contribution to the previously published work. The inclusion of the previously published work has the approval of the thesis or dissertation advisor and the Graduate Director.

Sincerely,

Dr. Katrina Groth
Director of Graduate Studies, Reliability Engineering
University of Maryland

Sincerely,

Michelle Bensi
Digitally signed by Michelle Bensi
Date: 2025.11.04 18:21:44 -05'00'

Dr. Michelle Bensi
Advisor for Joy Shen

Dedication

In honor of my mother, Mei-Yun Tuan; father, Song-Hua Shen, and brother, Yi Shen. You three were the foundation from which I was built. My tenacity and grit are a reflection of our love and care. I do it all for you.

加油!

Acknowledgments

Thank you to my advisor, Professor Bensi, for shaping me into a diligent and thorough researcher like yourself. I can't express my gratitude for all the hours spent on the live editing sessions, coding, as well as taking the time to draw out the bigger picture for me. I aim to be as dedicated to detail, transparency, and directness in my work and attitude as you are. I have equal thanks to give to my co-advisor, Professor Modarres, for taking me as your student, encouraging me to dive headfirst into reliability engineering. My excitement in pursuing my degree is directly from your passion and deep experience to contribute and teach in the reliability field. To be able to have both of you as my advisors and mentors is my pleasure.

I also thank Professor Groth, Dr. Siu, Professor Baecher, and Professor Al-Sheikhly for being on my dissertation committee, providing invaluable feedback on my proposal, and taking the time to review my dissertation. I especially thank Professor Groth for being an integral part of my graduate journey as a lecturer and supportive professor. Thank you, Dr. Siu, for keeping an open line of communication and always being willing to provide feedback and project opportunities aimed at explicitly honing my skills as a more well-rounded engineer.

I want to acknowledge the financial support from the Clark Foundation and funding from the Nuclear Regulatory Commission (NRC) under grant 31310021M0007. Any opinions, findings, and conclusions expressed in the dissertation are the author's and do not reflect the views of the research sponsor (NRC) or any other organization.

Finally, to my friends, I am lucky to have found a second family with you all. We are there for each other's successes and frustrations, always there to have a laugh or lend an ear. The endless nights of Mario party, binge-watching reality TV shows, and silly dinners where I had the privilege of enjoying our company got me through the thick of it. I want to thank Khalil Carrillo for always showing up when I need them the most (or least). To Navid Ashari, for being my emergency contact, my go-to phone call, my sounding board.

Table of Contents

List of Tables

List of Figures

List of Abbreviations

AEF	Annual exceedance frequency
ANS	American Nuclear Society
ASCE	American Society of Civil Engineers
ASME	American Society of Mechanical Engineers
BE	Basic event
BN	Bayesian network
CAP	Capacity
CCF	Common cause failure
CPT	Conditional probability table
DBA	Design basis analysis
DEM	Demand
ECB	Backward propagation evidence case
ECCS	Emergency core cooling system
ECF	Forward propagation evidence case
EDG	Emergency diesel generator
EPS	Emergency power system
ET	Event tree
FF	Flood failure
FG	Floodgate
FT	Fault tree
FTR	Failure to run
FTS	Failure to start
HCL	Hybrid causal logic
HCLPF	High-confidence-low-probability of failure
HRA	Human reliability analysis
LIP	Local intense precipitation
LOOP	Loss of offsite power
MC	Monte Carlo
MC-BN	Monte Carlo augmented Bayesian network
MSL	Mean sea level
NACCS	North Atlantic Coast Comprehensive Study
NPP	Nuclear power plant
NRC	Nuclear Regulatory Commission
PFHA	Probabilistic flood hazard assessment
PMF	Probable maximum flood
PMF	Probability mass function
PMP	Probable maximum precipitation
PMSS	Probable maximum storm surge

PRA	Probabilistic risk assessment
PS	Penetration Seal
RF	Random failure
RIDM	Risk-informed decision-making
SBO	Station blackout
SSC	System, structure, or component
TE	Top event
TM	Testing and maintenance
U.S.	United States
USACE	U.S. Army Corps of Engineers

Chapter 1. Introduction[1]

1.1 Context and Motivation

Nuclear power plant (NPP) sites are typically built near large bodies of water, such as rivers, lakes, or the ocean, for reactor cooling purposes. However, an NPP's proximity to these bodies of water increases its vulnerability to external floods.[2] Mohammadi et al. [2] estimate that all U.S. plants are exposed to local intense precipitation (LIP), 80% of plants can be affected by riverine floods, slightly over 40% are subject to storm surges, 40% are susceptible to dam failures, and 15% are potentially exposed to other various flood hazards.

An external flood can damage flood protection features, allowing water to infiltrate plant areas housing safety-related systems, structures, and components (SSCs). Flood-related operating experience has illustrated the potential challenges that can be caused by flood events. For example, in 2016 [3], heavy rainfall flooded a Japanese NPP reactor building through unsealed cable ducts. In the plant's first unit, the flood reached a room adjacent to a battery room. This flooding resulted in 6.6 tons of rainwater in the second unit, which was not considered a possibility nor included in the plant's design. In 2014, heavy rainfall at St. Lucie NPP in the U.S. [4] entered the auxiliary

[1] This introduction contains information from [1]

[2] External floods can be categorized as a phenomenon originating outside the plant that leads to the overflow or accumulation of water on or near the site [3].

building through degraded conduits that lacked internal flood barriers, flooding could have entered the emergency core cooling system (ECCS) pump room if operators did not close the ECCS sump isolation valves. In 2006, while Catawba NPP in the U.S. [5] was in shutdown, the emergency diesel generator (EDG) room was flooded through missing and degraded conduit sleeves from a maintenance hole due to a possible design, manufacturing, or construction/installation deficiency and inadequate configuration control of conduit/trench flood barriers. Notably, in 2011, the Tōhoku tsunami at the Fukushima NPP in Japan [6] overtopped seawalls, flooding the basement of the reactor and turbine buildings through building entrances, EDG intake louvers, SSC hatches, and cable and pipe penetrations, leading to damage of pumps, panels, batteries, and EDGs. In 1999, at Blayais NPP in France [7], floods overtopped seawalls and damaged dikes, allowing the flood to infiltrate critical areas through penetrations and doors. The flood affected rooms containing essential service water pumps, technical galleries, feeder SSC, safety injection pumps, and containment spray pumps. Additional examples of operating experience are documented in [8].

1.1.1 External Flood Probabilistic Risk Assessments in the Nuclear Industry

While external flood risks at NPP sites have been demonstrated in operating experience, external flood probabilistic risk assessment (PRA) modeling experience remains limited in the U.S. Because external floods are complex phenomena that arise from a range of phenomena and can lead to diverse site impacts, they are challenging to model within the conventional PRA

framework [9]. Additionally, there are limited data and statistical and modeling tools to represent external floods [10].

The current state of practice in analyzing external flood risks in the U.S. is largely concerned with screening methods or the deterministic approach of design basis analysis (DBA) [9]. DBAs establish that SSCs must be designed to withstand a design-basis flood based on historical data with a sufficient safety margin [10] [11]. The design-basis flood is typically represented by a deterministic probable maximum phenomenon or hazard level, defined as the most severe water level reasonably possible, given the conditions of the flood source and site location, exceeding the severity of all historically observed flooding events [11]. This concept is applied to a range of flood-causing phenomena and hazard levels, including probable maximum flood (PMF), precipitation (PMP), storm surge (PMSS), etc. Although the word 'probable' is used in this concept, it is a deterministic rather than a probabilistic analysis. The design basis flood level(s) is (are) compared to critical heights such as plant elevation, flood protection feature elevations, or SSC installation heights. The site is considered sufficiently designed not to fail against external floods if the design basis is at or below these critical heights [12].

The deterministic approach of DBAs has supported the nuclear industry in evaluating (and reevaluating) the plant's ability to withstand external floods. However, the U.S. Nuclear Regulatory Commission (NRC) has expressed the need to increase efforts to use risk-insights to become modern regulators [13]. Particularly, the NRC issued a policy statement [14] that calls for

the integration of probabilistic methods and data, such as a PRA, to complement the deterministic approach in analyzing plant risks.

The probabilistic approach enhances deterministic methods of interpreting risks by considering a broader set of safety challenges, providing a systematic means to prioritize challenges based on probabilistic risk significance, and allowing the consideration of a more comprehensive set of resources to defend against these challenges [15].

1.1.2 Conventional Probabilistic Risk Assessment

PRA is the quantitative tool by which plant risk insights are developed. PRAs reflect the current knowledge of a plant's design, operation, and environment [15]. A PRAs objective is to answer the fundamental questions in the risk triplet [16]: (1) What can go wrong? (2) How likely is it? and (3) What are the consequences? The answers to the risk triplet guide practitioners in generating possible risk scenarios, assessing their frequencies, and determining the expected consequences. PRAs have generated risk information for safety and regulatory decision-making in the nuclear industry since the 1970s with the publication of WASH-1400 [17].

Most PRA efforts in the U.S. develop level 1 PRAs with conventional risk tools, such as event trees (ETs) and fault trees (FTs), to model and quantify accident scenarios in binary states. The effort in PRA development has resulted in a robust foundation of experience and knowledge in analyzing the impact of internal events on plant systems. However, there is increasing interest

in expanding the PRA scope to external hazards such as external floods. However, external floods have been largely screened out from external hazard PRAs performed to date, and, as a result, few comprehensive external flood PRAs have been performed in the U.S.

Furthermore, the static treatment of time in existing PRA approaches precludes the flood's dynamics from being fully captured in conventional tools. Currently, static risk tools capture the evolution of an event through the accident sequence, the order of which is determined through functionality, and do not capture the evolution of the flood in time and space. This work focuses on increasing the realism in modeling the flood's temporal and spatial dependencies through causal modeling.

The American Nuclear Society (ANS) and American Society of Mechanical Engineers (ASME) have jointly developed an external hazard PRA standard for guidance [18]. The external flood standard is structured around the development of a PRA that consists of three key elements [18]: (1) probabilistic flood hazard assessment (PFHA), (2) flood fragility evaluation, and (3) plant response model. PFHAs characterize and quantify the external flood hazard probabilistically (e.g., frequency and severity) at a given site. The flood is typically represented through a flood hazard severity metric such as flood height or velocity, depending on the needs of the PRA. The results of a PFHA are typically presented as a hazard curve, providing the annual exceedance frequency (AEF) of a measure of flood severity. The flood fragility evaluation assesses the capacity of flood protection features to withstand the flood's demands [19]. Fragility is typically expressed as the

conditional probability that a flood protection feature reaches or exceeds a damage state, given the flood demand [19] [20]. The fragility evaluation may involve converting flood severity to a flood demand variable that is relevant to SSC response, such as converting flood depths to hydrostatic pressure [21]. There are four main approaches to developing fragility functions [22]: empirical, analytical, engineering judgment, and a hybrid approach. The empirical approach develops fragility functions through in situ and experimental observations. The analytical approach develops fragility functions through the definition of limit state functions. The engineering judgment approach quantifies fragility through subject matter expertise. A hybrid approach includes combinations of the previous approaches. The plant response assessment models the accident sequences and component failure combinations, informed by the PFHA and fragility evaluation results. The plant response is typically represented with ETs and FTs, which are structured and quantified using Boolean algebra [23]. ETs model potential accident scenarios that lead to an undesirable condition in response to an initiating event (i.e., a challenge to plant operation). Accident scenarios consist of several "pivotal events" or undesired states of the system. These events are deductively expanded into more basic component failures, maintenance, and human errors using FT analysis to model and quantify failure combinations that lead to the occurrence of the pivotal event. Functional dependencies are represented in the ET's and FT's logic, while common cause failures (CCFs) are a basic event that represent failures among identical SSCs due to a particular root cause and coupling factor [24].

1.2 Research Needs

Incorporating a complementary probabilistic approach with the deterministic approach can enhance insights into flood risks and improve the development of mitigation strategies. However, existing probabilistic methods that rely on ETs and FTs have limiting assumptions in binary states, static treatment of time, and spatial homogeneity across the site. Binary states can obfuscate partial damage states on the plant's overall ability to withstand the flood. The static treatment of time and spatial homogeneity does not explicitly capture the flood's evolution over the flood's duration and across the site. These assumptions challenge external flood modeling as floods are a dynamic phenomenon in which their effects and propagation are not consistent throughout the event or site. These challenges prompt the investigation of alternative modeling tools.

1.2.1 Research Objectives

To address the identified research need, this dissertation aims to develop a novel modeling approach that meets the following objectives:

- **Objective 1**: Leverages a probabilistic approach that incorporates how flood hazards physically impact the site.
- **Objective 2**: Captures relevant external flood modeling considerations that are not explicitly included in conventional modeling approaches, such as temporal, spatial, and CCFs, and multiple damage states.
- **Objective 3**: Strategies to interface the novel framework with conventional ETs and FTs and compare the advantages and challenges in each strategy.

1.3 Research Approach

The three objectives are accomplished in this dissertation by first investigating the current state of practice of conventional risk tools in flood applications through a literature review and issuance of a questionnaire to collect insights regarding needs and trends related to PRA modeling within the nuclear industry, which are both provided in Chapter 2. These insights informed the modeling approach described in this dissertation, which centers on a Bayesian network (BN) that has been augmented by a Monte Carlo (MC) simulation, referred to as an MC-BN. In an effort to preserve the foundation of knowledge and experience in ETs and FTs, while leveraging the benefits

of the MC-BN, this dissertation explores strategies to interface the MC-BN with conventional tools to form a hybrid approach as seen in Figure 1.

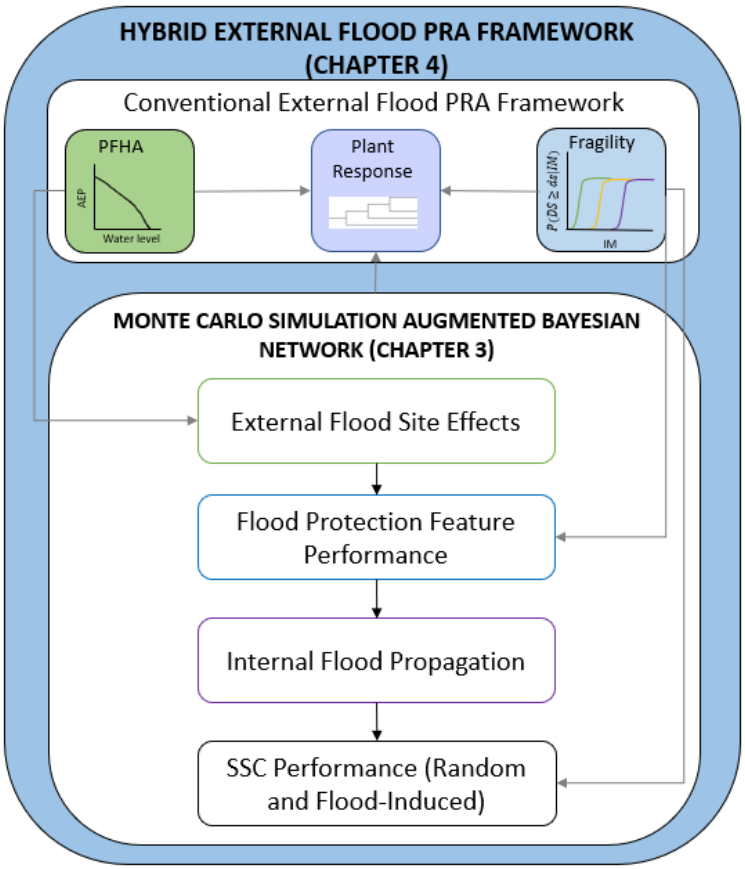

Figure 1: Hybrid External Flood PRA Framework

Discussed in Chapter 3, the MC-BN is structured on the logic of the external flood pathway, beginning with an external flood propagated across the site and potentially impacting flood protection feature performance. Depending on flood protection performance, the external flood can propagate inside structures and affect the performance of SSCs within the flooded zones.

In Figure 1, the BN is interfaced with ETs and FTs, forming the hybrid external flood PRA model. As there are advantages and limitations to delegating the external flood modeling and random failures to either the MC-BN, ETs/FTs, or a combination of either, multiple configurations are investigated. The quantitative and modeling characteristics of both the MC-BN and ETs/FTs in this dissertation are demonstrated on a case study of a representative NPP site.

Chapter 4 summarizes the work accomplishing the objectives and their contributions to improving the assessment of external flood risks at NPPs, as well as future work.

Chapter 2. Insights Regarding Current Probabilistic Risk Assessment Technologies for External Flood Risk-Informed Decision Making

Conventional PRA tools of ETs and FTs have enhanced practitioners' understanding of plant systems and risks. However, challenges arise when using conventional risk tools in the context of external flood PRA. Specifically, the sections that follow summarize a literature review on challenges in characterizing an external flood and key assumptions in conventional risk tool modeling in an external flood PRA context.

2.1 Identification and Assessment of Current and Developing Probabilistic Risk Assessment Technologies Obtained through a Questionnaire[3][4]

The needs of the PRA community have evolved since the original tools were developed. However, technologies and algorithms available at the time limited these legacy tools. Current technologies have improved in computational power and capabilities, potentially enhancing the ability to model plant risks, especially regarding external hazards. The advancements of new tools and technologies require a re-analysis to discuss their advantages and limitations, potential

[3] Contents of this Section was presented in [25]

[4] Questionnaire details are provided in Appendix B: Conditional CCF Discussion and Example.

contributions to external hazard PRAs, and effects on the risk-informed-decision-making (RIDM) process.

A questionnaire on PRA tools in the nuclear industry was created to understand practitioners' insights on the advantages/limitations of existing tools and how other tools supplement the conventional PRA model, the details of which are provided in [25]. This work synthesizes and presents feedback, supplemented with a review of existing literature, to develop a comprehensive analysis of the current state of practice on PRA tools and other tools in the nuclear industry.

The responses offered diverse insights due to differences in the user's experience, which in some cases led to contradictory responses or commentary that did not reflect the capabilities of current tools. The conflicting responses prompted engagement with vendors and developers of conventional PRA tools to clarify their respective tool capabilities [26]. Respondents recognized that tools have improved since the initial development of legacy tools. Tools have also enhanced the users' experiences by migrating from command-driven interfaces to menu-driven or graphical user interfaces and providing better training documentation. This potentially reduces the learning curve and setup time that may have previously acted as a barrier to entry into the PRA community. As previously mentioned, there are inconsistencies in views regarding the advantages and limitations among respondents. Quantification efficiency and comprehensiveness/ incomprehensiveness of tool capabilities are the significant functionalities that are inconsistent among respondents due to subjectivity. According to the respondents, the lack of dynamic and

post-processing capabilities is the main gap in current tools. Tool capabilities have expanded for external hazard PRAs, which require additional functionalities to perform external hazard analyses, fragility function development, and plant response. However, respondents have expressed that those functionalities need to continue to improve external hazard integration and analysis modules to develop a full scope external hazard PRAs. Although dynamic tools exist, the most common PRA tools were not designed to integrate a temporal component. Post-processing capabilities are limited due to the diverse options for presenting and sharing results. Currently, general-purpose tools such as Python, MATLAB, and Excel are best suited to allow users to convey results to other PRA practitioners, stakeholders, and decision-makers. External hazard scopes vary and require a diverse set of analyses. This poses a potential issue for tool developers in evolving tools to fit the community's needs for external hazard PRAs. Similarly, external tool interfacing has been enhanced, but there is still a gap noted among respondents in the comprehensiveness of software integration. Current tools excel in efficient quantification and fast setup of large and complex models, utilizing the availability of advanced computers and efficient algorithms. Quantification efficiency is still a source of disagreement among the respondents. It should be noted that the insights on quantification efficiency are especially dependent on the practitioners' model complexity and the capabilities of current technologies.

Respondents indicated that the scope of PRAs has expanded into level 2 and 3 PRAs and requires internal and external hazard analyses. This scope expansion will increase the need for new tools and model complexity, necessitating a re-evaluation of how system failures are viewed and

treated, and continuing the advancement of algorithm and tool capabilities. Respondents expressed interest in integrating CCF analyses, as there are many identical SSCs, and NPP sites are multi-unit. Component aging and degradation analyses are also required for practitioners, as it is essential for external hazards in understanding pre-existing conditions (before the flood) in failure data. A few respondents acknowledged that human reliability analysis (HRA) has a limited scope in external hazard PRAs, but it is necessary, especially for hazards with significant warning time, temporary measures, and loss of site access. Respondents also noted that the modernization of nuclear technology and increased users in the global community would increase collaboration. They highlighted the need for improved model management, such as the ability for multiple users to work on a model with version control capabilities simultaneously, the use of digital twins, and model traceability to improve the ability for collaboration. There is an increased emphasis on including dynamic capabilities. Respondents expressed interest in tool integration to facilitate multi-scoped software that can address the needs of multi-level, multi-unit, and multi-hazard PRAs. Although it is acknowledged that the increased scope may impede software computational speed and model setup.

Hybrid combinations of conventional, novel, and additional PRA tools are increasingly used to address the evolving needs of the PRA community. A questionnaire on PRA tools was created to understand practitioners' general insights on the advantages/limitations of existing tools and how other tools supplement conventional PRA models. In response to the questionnaire, nearly all respondents highlighted advancements in algorithm efficiency, software compatibility, and ease of

use. Incorporating new computational algorithms within the tools has reduced computational speed and capabilities, increasing the convenience of developing models. Integrating comprehensive functionalities and interfacing with other tools has facilitated the expansion of the PRA scope to external hazards. The questionnaire highlights the trends that the respondents would like to see the technology evolve towards, such as dynamic PRA capabilities and collaboration functionalities. The technology has the potential to also expand the traditional scope of RIDM in the nuclear industry by diversifying the identified issues and their mitigation options. It allows practitioners to analyze a wider variety of accidents and allows stakeholders to prioritize accident mitigation, informed by a realistic model. These tools are critical in optimizing decision-making by testing key assumptions and providing information and insights.

The engagement with PRA professionals highlighted five key challenges in PRA modeling. This dissertation specifically incorporates the bolded bullet points.

- **Improve HRA modeling.**
- **Improve SSC dependency modeling.**
- **Incorporate Bayesian updating.**
- **Incorporate dynamic PRA modeling.**[5]
- Expand the PRA scope to external events.

2.2 Spatial Homogeneity Assumption in Probabilistic Flood Hazard Assessments

Flood events can affect an entire NPP site, which results in spatial flood-induced dependencies in the loads imposed upon SSCs. As the flood propagates across the site, it can affect multiple SSCs by imposing loads over a given duration that may be similar but not necessarily identical, generating dependencies in which these loads will be partially or completely correlated [27]. Because of the spatial variability in flood effects across the site, these loads could be completely, partially, or not correlated. Other sources of correlation in SSC performance include similarities in

[5] While dynamic PRAs are valuable in modeling system dynamics, a full-scope dynamic PRA is out of the scope of this work. Dynamic considerations of the external flood will be incorporated through temporal dependence.

design, construction/installation, maintenance, and degradation, as well as shared support infrastructure.

PFHAs traditionally analyze the propagation of external floods across the site with complete dependence, meaning that the flood hazard associated with a given AEF results in constant severity (e.g., flood elevation) throughout the site [28]. However, partial dependencies can couple systems due to topographic differences across the site, and SSC elevations can lead to differences in flood severity across the site during a flood event. This assumption can challenge the model's accuracy when the hazard is assessed locally within the site. Neal et al. [29] employed an MC simulation on a hydraulic model to account for realistic spatial dependencies in the areas between tributaries with a 10-meter resolution. Quinn et al. [30] applied multivariate extreme statistical models to account for spatial dependencies within large regions computed with a series of pairwise regressions. Winter et al. [31] compared spatial dependency modeling using two different approaches: multi-site peak flow dependence modeling and a weather-generator-based approach. The literature on modeling spatial dependencies in PFHAs has provided methods to account for spatial dependencies. However, it has yet to be applied to assessing the flood's impact on flood protection features. Additionally, the research employs computationally expensive methods that account for topography and meteorology.

2.3 Static Treatment of Time in External Hazards

Conventional static PRA scenarios treat time implicitly through approximate chronological success and failure of SSCs in the accident sequence. However, hazards such as floods evolve with varying magnitude and thus varying impact on the site. Dynamic analyses can improve upon static PRAs by explicitly modeling time and capturing the accident progression and system status evolution [32]. These considerations apply to external floods as they are a heavily time-dependent phenomenon, evolving in magnitude and space.

Dynamic PRAs have become an increasingly researched area in nuclear power PRA using methods such as direct simulation, state-transition models, and dynamic ETs [33]. However, comprehensive dynamic PRAs have high computational demand and modeling requirements. There is research in developing hybrid approaches with static and dynamic PRA tools to address the shortcomings of the static treatment of time by extending conventional tools to explicitly model time values or states [34], [35], [36] . These hybrid approaches have provided a foundation for integrating static and dynamic methods. However, they have yet to be applied to external flood modeling, which has spatial considerations that are temporally dependent. This work focuses on improving static methods by integrating dynamic considerations through temporal dependencies, which have been applied outside of the nuclear industry in external hazard analyses. Apel et al. [36] used a bivariate normal distribution to analyze the joint distribution for flood peaks and flood volumes, as well as flood volumes and flood durations. This model utilized the Box-Cox

transformation method to normalize the distributions of flood peaks, volumes, and duration. Yue et al. [37] proposed the use of a Gumbel mixed model, which was a bivariate extreme value distribution model with Gumbel marginals, to analyze the joint probability distribution of correlated flood peaks and volumes and flood volume and duration. Zhang and Singh [38], Latif and Mustafa [39], and Liu et al. [40] used copulas in their studies to derive flood frequency distribution models for various flood variables such as flood peak, duration, and volume. This dissertation on the joint probabilistic distribution of flood duration and other relevant intensity measures provides more realistic PFHA results. However, these multivariate flood hazard models have yet to be applied to a framework to assess the impact on flood risks. There is work in modeling the impact of flood duration and flood height on flood disaster risks using BNs by Wu et al. [41] and Harris et al. [42]. However, flood height and duration are not conditioned on each other, preventing the analysis from modeling the temporal dependencies. The current state of PFHAs provides an opportunity to develop a framework to model the causal relationship between flood height and duration.

2.4 Binary Damage State Assumption in Component Flood Performance

Traditionally, component performance under flood effects is assumed to be binary, i.e., either not failed or failed, when a flood reaches a specified elevation. For example, Kohut [43], Siu et al. [44], and Ebisawa et al. [45] discuss the assumption that components are typically assumed to fail when the flood level reaches the installation height. This binary approach leads to stepwise fragility

functions and is generally appropriate for overtopping or brittle failure modes and well-understood capacities. However, there is increasing experience in developing smoother fragility functions, which are more suitable for elastic and complex SSCs, as well as when there is uncertainty regarding component performance.

A limited number of studies have addressed the fragility of NPP flood protection features. Pope et al. [46] conducted various experiments on hollow-core and steel door fragilities using a full-scale interior door apparatus with different configurations. The set of experiments collected failure data on leakage, flood height, and inlet flow rate, applying Bayesian regression to estimate parameters for lognormal and Weibull distributions to model flood fragility functions. These experiments provide an opportunity to expand on fragility development for other flood protection features, such as penetration seals, floodgates, and different door configurations. Kozlik [47] and Kaida et al. [48] assume the fragility function for the failure damage state is normally or lognormally distributed, respectively, against flood levels. Research is needed to expand on damage states and develop functions for intermediate damage states.

Outside of the nuclear industry, there is a considerable effort to understand the fragility of flood defense structures. Allsop et al. [49] compiled documentation on failure mechanisms and capacity for various flood defense structures such as foreshores, dunes, and banks, embankments and revetments, walls, and point structures for various hydraulic loadings. However, these capacity

equations are not appropriate for flood protection features located on a building envelope, such as doors, floodgates, and penetration seals.

2.5 Hybrid External Flood Probabilistic Risk Assessment Approach

Hybrid PRA frameworks with BNs have been leveraged to model risk and reliability for NPPs. For example, Lee and Lee [50] leveraged BN inference with traditional PRA sensitivity methods to predict the evolution of environmental conditions of waste disposal facilities. Segarra et al. [51] leveraged BNs for multi-unit seismic PRAs to account for spatial dependencies across reactor units. Tolo et al. [52] developed an enhanced BN to quantify the risk of flooding hazards in spent nuclear storage facilities. Their proposed BN accounts for climate change predictions, external hazard effects on internal subsystems, and human error, mainly processing imprecise random variables. Garcia-Herrero et al. [53] applied BNs to model soft variables from organizational culture and safety culture effects on NPPs. Groth et al. [54], Wang [55], and Mosleh et al. [56] have developed and applied a hybrid causal logic (HCL) model that links event sequence diagrams and BNs to model risk scenarios, system risks, hazards, and soft causal factors from human and organizational factors. This precedent has established BNs as a robust and advanced risk assessment tool for various applications. However, a hybrid framework has yet to be applied to an external flood context.

These assumptions in spatial homogeneity, static treatment of time, and binary damage states can impose simplifying strategies to external flood PRA modeling, decreasing the transparency of

the flood model. This study proposes using a BN as a means of modeling external flood-induced, spatial, and temporal dependencies. In addition, BNs are a convenient tool for external flood modeling because BNs can expand the binary component state assumption to multiple states. Furthermore, the BN is flexible, and its results can be easily integrated into an ET/FT through Boolean logic.

Chapter 3. Monte-Carlo Augmented Bayesian Network Approach to External Flood Risk Modeling [6]

This study develops an MC-BN that incorporates technical modeling insights and challenges from the PRA community engagement from Section 2.1 and addresses the challenges discussed in Sections 2.2 to 2.4. A brief introduction to BNs is provided in Section 3.1.

3.1 A Brief Introduction to Bayesian Networks and Inference

BNs are comprised of nodes (circles) that represent random variables and directed links (arrows) that represent the dependence between them. Typically, the direction of the links reflects a causal interpretation. An example of a BN is shown in Figure 2.

[6] This chapter presents a modified version of the work published in [1]

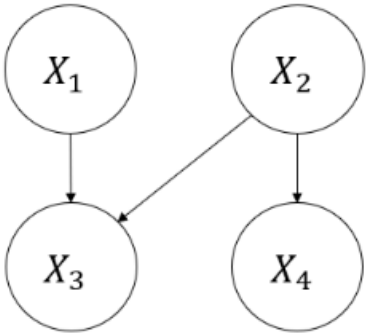

Figure 2: Example BN

The BN in Figure 2 consists of four nodes, each representing one of four random variables, X_i $i = 1, \ldots, 4$. The directed links connect each node represent their probabilistic dependence. BNs use familial terminology to describe the dependencies between nodes. X_3 is the *child* node to its *parent* nodes, X_1 and X_2, as indicated by the directions of the directed links. Additionally, X_4 is also the child node of X_2, X_1 and X_2 are also considered root nodes as they are not probabilistically dependent on other variables. Quantitatively, each node is associated with a conditional probability table (CPT), quantifying the probability of the child node's states given the mutually exclusive states of its parent node. Consistent with many risk tools used in risk assessments, random variables represented in BNs are typically modeled as discrete (though continuous random variables can be used in unique circumstances [57], [58], [59]).

3.1.1 Bayesian Inference

Bayesian inference refers to using a BN to answer probabilistic queries on a problem context by propagating evidence with the conceptual application of Bayes' rule [60]. Efficient inference

engines and algorithms, such as the elimination or junction tree algorithms [61], are often used for inference in Bayesian tools. Inference enters evidence at one or more nodes, updating the probabilities of all other nodes. The probabilities can either be updated by forward inference, backward inference, or some combination [62].

Forward inference is predictive, propagating evidence in the direction of a directed link or from cause to effect. This inference type inserts evidence at a parent node, propagating the information to its child nodes. Backward inference is diagnostic, propagating evidence in the opposite direction of a directed link or from effect to cause. This inference type inserts evidence at a child node, propagating the information to its parent nodes. For an introduction to BNs in an external hazard context, refer to the work of Bensi [61] and Segarra [63].

3.2 Monte Carlo Augmented Bayesian Network for External Flood Modeling

This dissertation seeks to incorporate technical modeling insights from the PRA community engagement and address challenges in probabilistically modeling an external flood impacting a site. Specifically, this study proposes an MC-BN, leveraging its ability to incorporate temporal and spatial dependency modeling to characterize the flood. Specifically, the MC-BN can incorporate causal dependencies that capture how the flood level may vary across the site and uncertainty in the duration of effects. While dynamic PRA tools have made significant efforts and contributions to modeling an evolving PRA, this work seeks to develop an intermediate framework that introduces dynamic considerations through causal modeling.

The BN can also improve upon the conventional limitations in modeling multiple component states and improve upon SSC dependency modeling. Furthermore, BNs have the benefit of Bayesian updating, providing meaningful insights into the system's response to variable states. However, BNs can become complex and computationally expensive, requiring a high memory demand. In addition, BNs are typically discrete or discretize continuous random variables, which can lead to discretization errors. This study augments the BN with an MC simulation to quantify functions of random variables (e.g., limit state functions), reduce memory demands and discretization errors, and generate the CPTs in the BN. This multi-method approach seeks to expand on the current flood risk modeling capabilities while managing tool challenges in memory demand.

Within the context of external flooding, the proposed MC-BN meets three main research objectives:

- Objective 1: Model hazard variability across a site and capture some temporal factors.
- Objective 2: Model the multi-state performance of a diverse set of flood protection features and components.
- Objective 3: Estimate the probability distribution of internal flood depths, accounting for relevant variables associated with Objectives (1) and (2).

The proposed modeling approach reflects a strategy for probabilistically mapping external flooding hazards at a reference location to an internal flood depth, accounting for spatial variability and the performance of flood protection features. An analog can be drawn between the proposed approach and seismic hazard-specific strategies for modeling site response (which models how ground motion is affected by site characteristics) and in-structure response (which captures how seismic motions are altered as they move through a structure) as part of the fragility assessment.

3.3 Development of the Monte-Carlo Augmented Bayesian Network

The generalized MC-BN shown in Figure 3 models an external flood impacting an NPP building envelope consisting of n flood protection features. A summary of each node category and constituent node (random variable) descriptions is provided in Table 1.

A site reference hazard (root node of the BN) is characterized by a flood severity metric and is dependent on flood duration. Then, each flood protection feature's performance (blue nodes) against the location-specific flood demand (green nodes) determines whether floodwater flows through the features (purple nodes). When flood waters enter the building, the resulting internal flood depth in the building is modeled based on the cumulative flow through the features, which is shown as the converging structure at the bottom of the BN. This section provides a high-level overview of developing each node in Figure 3, and implements the case study in the following section.

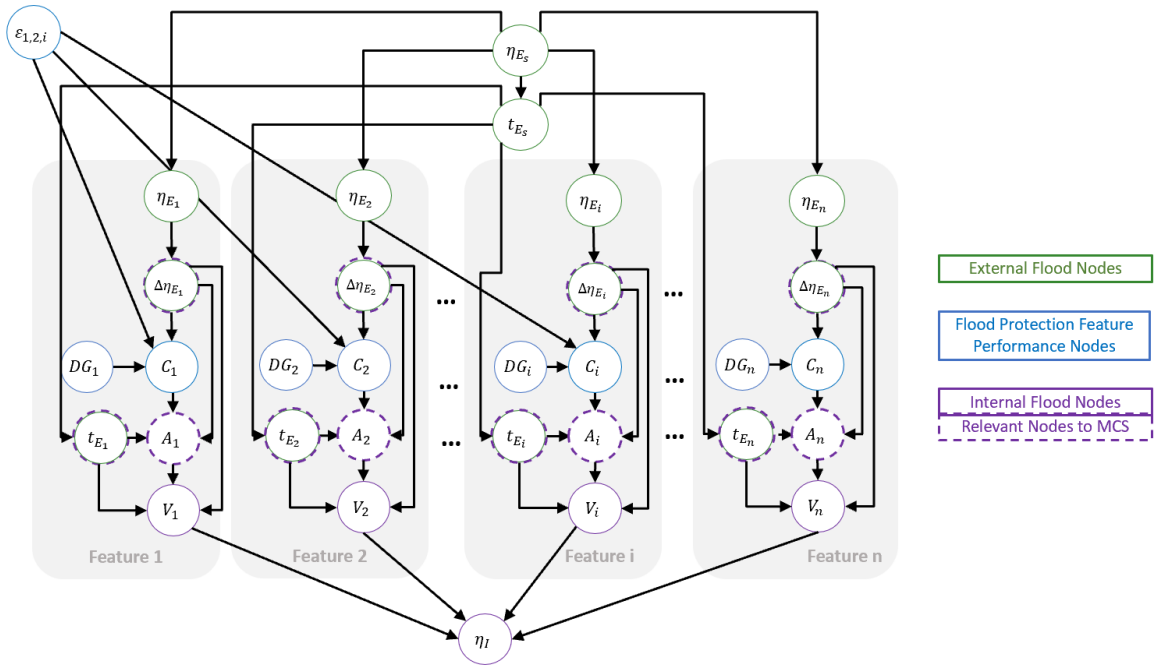

Figure 3: General External Flood BN

Whenever the BN includes continuous random variables and functions thereof, MC simulation generates the requisite CPT as described in [64]. In addition, MC simulation is used to eliminate some nodes in the BN as a means of reducing demands and discretization errors. This study initially presents the complete BN (Figure 3) in Section 3.3 and outlines the MC augmentation of the BN (Figure 6) in Section 3.3.7 in which relevant internal flood nodes outlined by the dashed purple outline are integrated out of the BN through MC simulation and are distinguished with a single asterisk (*) in Table 1. Note that elevations in this illustrative study are assumed to be relative to mean sea level (MSL) in meters but can be defined as appropriate given the site's characteristics.

Table 1: Node Categories and Node Descriptions

Node group	Random Variable	Units	Description
External Flood	η_{E_s}	(m) MSL	Flood elevation at the site reference location with respect to a reference datum
	$\eta_{E\,i}$	(m) MSL	Flood elevation at the location of flood protection feature $i = 1,2, \dots, n$
	$\Delta\eta_{E_i}{}^*$	m	Flood demand on flood protection feature $i = 1,2, \dots, n$
	$t_{E_s}{}^*$	s	Duration of external flood at the site reference location
	$t_{E_i}{}^*$	s	Duration of external flood at location of flood protection feature $i = 1,2, \dots, n$
Flood Protection Performance	DG_i	--	Pre-existing degradation state of flood protection feature $i = 1,2, \dots, n$
	ε_i	--	Fragility error associated with flood protection feature $i = 1,2, \dots, n$
	C_i	--	State of flood protection feature $i = 1,2, \dots, n$
Internal Flood	A_i	m^2	Cross-sectional area of flood protection features $i = 1,2, \dots, n$ lost due to damage
	$V_i{}^*$	m^3	Flow volume through flood protection feature $i = 1,2, \dots, n$
	η_I	m	Internal flood depth within the structure

3.3.1 External Flood Nodes

The external flood nodes $\eta_{E_S}, \eta_{E_i}, \Delta\eta_{E_i}, t_{E_S}$ and t_{E_i} represent random variables that model the external flood across the site. Key quantities used to define the external flood elevations and demand nodes are illustrated in Figure 4, which depicts a cross-sectional view of an NPP site with variable site features, consisting of a single building envelope. The envelope in Figure 4 consists of a single flood protection feature (shown by the white circle).

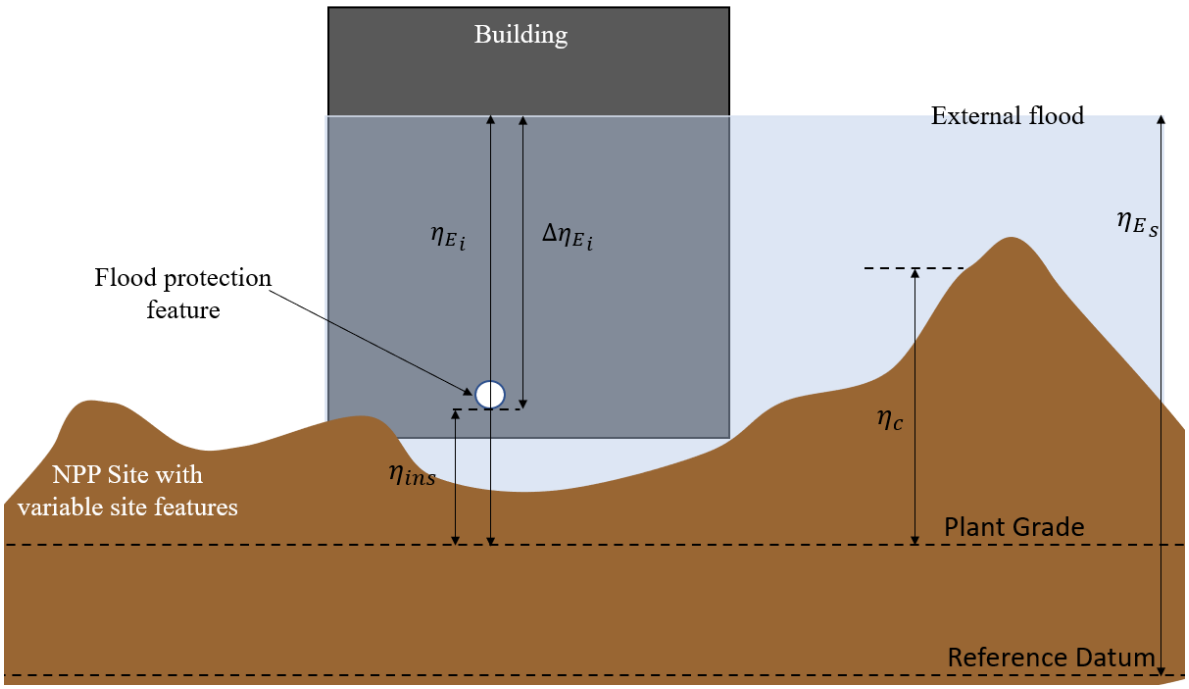

Figure 4: Illustrative Diagram of Building Envelope for Flood Protection Feature Demand Calculations

Node η_{E_S} represents the external flood elevation at the site reference location s, measured against a reference datum, or as MSL in this case. As mentioned in Section 1.1.2, a PFHA can yield a hazard curve that provides the AEF[7] associated with a range of flood severities [65]. PFHA frameworks are described in existing references, such as Prasad and Meyer [66] and Kanney et al. [67]. The states of node η_{E_S} are determined by discretizing the hazard curve into specified ranges, often known as flood hazard bins or flood intensity bins. The marginal probabilities of η_{E_S} are assigned to each discretized state of the hazard curve.

Assuming static forces, the external flood elevation node η_{E_S} is the parent to nodes representing the location-specific flood elevations η_{E_i} which represents the local elevation of the flood at the location of flood protection feature i. The transformation from η_{E_S} to η_{E_i} can be calculated using a range of approaches, such as the modified flow-tub approach as seen in the cross-sectional diagram in Figure 4. The flow-tub approach models floodwaters with hydraulic connectivity from the flood source and path-based attenuation [68]. In the figure, η_c is the top elevation of a feature, such as a flood wall, which may impede or block the flood from reaching the building. This transformation captures the site's features or configurations by modeling the spatial dependency in which the flood may be impeded or stopped from reaching features of

[7] Conventional flood hazard literature may use AEF and annual exceedance probability interchangeably. This study differentiates between frequency and probability. This dissertation defines AEF as the annual rate of a flood occurring with severity greater than or equal to a specified threshold.

interest. η_{E_S} is also parent to a node representing the duration of the flood at the site reference location, t_{E_S} which in turn are parent nodes to location-specific duration t_{E_i}. Conditioning the duration on external flood height introduces some dynamic considerations that reflect how the time SSCs are exposed to flood levels may vary as a function of flood level.

Location-specific flood elevation nodes are parents to the associated external flood demand nodes $\Delta\eta_{E_i}$ which represent the flood's demands imposed on flood protection feature i. For example, in Figure 4, flood elevation η_{E_i} is transformed to a flood demand on the flood protection feature $\Delta\eta_{E_i}$ by taking the flood depth above the feature installation elevation η_{ins_i}, which is measured from the reference datum to the bottom of the feature; $\Delta\eta_{E_i} = \eta_{E_i} - \eta_{ins_i}$ if $\eta_{E_i} \geq n_{ins_i}$ or zero otherwise. It is noted that this formulation does not account for the effects of groundwater on features located below grade.

3.3.2 Flood Protection Feature Performance Nodes

Flood protection feature performance nodes DG_i, ε_i, and C_i characterize flood protection feature i's ability to withstand a flood demand. The flood protection feature performance is characterized by a flood fragility represented by a median capacity (based on a protection feature's pre-existing degradation state) and fragility error. Flood protection feature state C_i models the damage state of the flood protection features and has three parent nodes: flood demand $\Delta\eta_{E_i}$,

described in the previous section, as well as fragility error ε_i and pre-existing degradation state DG_i, discussed in the following sections.

3.3.3 Pre-Existing Degradation State Nodes DG_i

The node DG_i models the pre-existing degradation state of flood protection feature i and captures the probability of pre-existing damage or degradation, such as corrosion, wear, improper maintenance, etc., incurred before the flooding event. The pre-existing degradation can physically deteriorate the flood protection feature's capacity to withstand the demand. This deterioration is incorporated in the proposed model through a pre-existing degradation factor $P_{i,k}$ on the feature's median capacity (though the model can be extended to capture the effect of degradation on the uncertainty in the capacity as well). The marginal probabilities and node states can be sourced from plant walkdowns or experimentation. However, existing experimental data is limited [69].

3.3.4 Flood Protection Feature State Nodes C_i

The node C_i models the performance of the flood protection features i during the flood. The states of the component's performance are established through damage states k which represent the severity of damage experienced during the hazard event. Damage states are defined based on empirical data, engineering judgment, or operational events. However, defining these states is a non-trivial task for realistic analyses, as it depends on consequences and timing. The damage state, k, may be characterized by the limit state function, which can be conceptualized as

the ability of the capacity of feature i to resist damage state k ($CAP_{i,k}$) and demand imposed on the feature (DEM_i). The limit state function is expressed as a ratio of capacity to demand. The failure of component i for damage state k is determined if the limit state is less than one, as quantified in Equation 1.

$$g_{i,k}\left(X_{i,k}, \theta_{i,k}, DG_i\right) = \frac{CAP_{i,\mathrm{k}}\left(X_{i,k}, \theta_{i,k}, DG_i\right)}{DEM_i(\mathrm{X}_{i,k})} \leq 1 \qquad \text{Equation 1}$$

where $g_{i,k}(X_{i,k}, \theta_{i,k}, DG_i)$ is the limit state function for damage state k of feature i, $\mathrm{X}_{i,k}$ is a vector of random variables that influence the capacity and demand of feature i to resist damage state k, $\theta_{i,k}$ is the vector of parameters that define the limit state function, and DG_i reflects the deteriorating effect of the pre-existing condition on feature i's capacity to resist damage state k.

More formally, using a limit state function, the fragility function can be defined as the conditional probability of the demand exceeding the capacity (i.e., $g_{i,k}(X_{i,k}, \theta_{i,k}, DG_i) \leq 1$), given the hazard severity measure:

$$F_{i,k}(s_i, \theta_{i,k}, DG_i) = \Pr[\{g_{i,k}(X_{i,k}, \theta_{i,k}, DG_i) \leq 1\} | S_i = s_i] \qquad \text{Equation 2}$$

where $F_{i,k}(s_i, \theta_i, DG_i)$ is the fragility as a function associated with damage state k and feature i, as a function of hazard severity at the location of feature i, S_i and pre-existing degradation state DG_i. Damage states are sequential, mutually exclusive, and collectively exhaustive. Therefore, the

cumulative probability across all damage states at a given severity measure sums to one, and each probability can be computed through the difference of sequential damage states, as seen in Figure 5.

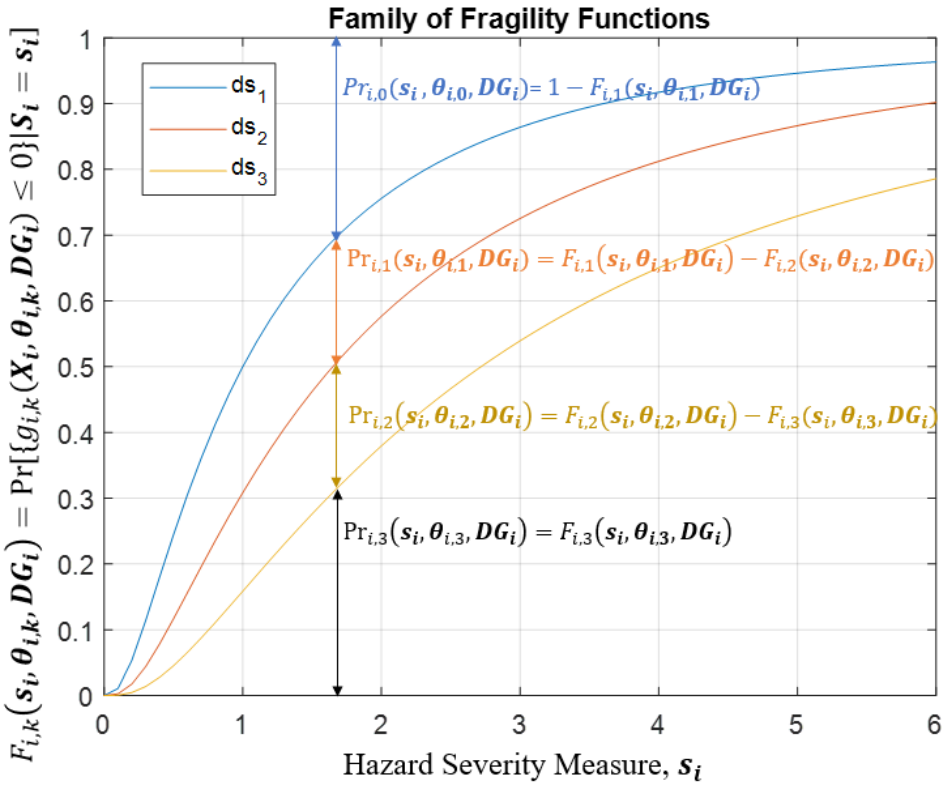

Figure 5: Example of a Family of Fragility Functions and State Probabilities with Four Damage States (adapted from [19]*)*

3.3.5 Fragility Error Nodes ε_i

There is limited literature on flood fragilities, particularly for building envelope flood protection features. This study uses median capacity and uncertainty values to model the ability of the feature to withstand the demand. Median capacities can be obtained, for example, through experimentation or technical specifications from manufacturers. Since median capacity, $\Theta_{med,i,k}$, is a deterministically defined parameter, a fragility error term is included to capture the aleatory variability (or uncertainty) and epistemic uncertainty [63] about the median. This study adapts the typical formulation [70] of capacity of feature i to withstand damage state k as:

$$CAP_{i,k} = (\Theta_{med,i,k} * R_{i,k}) \cdot \varepsilon_i = (\Theta_{med,i,k} * R_{i,k}) * (E_R * E_U) \qquad \text{Equation 3}$$

where flood capacity $CAP_{i,k}$ is the product of a best-estimate median capacity ($\Theta_{med,i,k}$) multiplied by a pre-existing degradation reduction factor $R_{i,k}$ associated with degradation state DG_i on the capacity of feature i to resist damage state k. ε_i is a normally distributed error term that encompasses both aleatory (random) variability E_R and epistemic uncertainty E_U. Portions of this error are common across components with similar characteristics, leading to a correlation in flood protection feature performance [63]. This is reflected in Figure 3 by the error nodes that are parents to multiple flood protection features. The fragility error CPTs required in the BN are obtained by discretizing the error distribution.

3.3.6 Internal Flood Nodes

The internal flood is characterized by a physical relationship reflecting the flood demand and duration, generating a flood volume that penetrates the building envelope through a flood protection feature's cross-sectional area loss (defined by the feature's performance). MC Simulation is leveraged to integrate out nodes from the BN through consideration of physical phenomena relevant to V_i.

3.3.7 Relevant Nodes to Monte Carlo Simulation Integration into Node V_i

In Figure 3, V_i represents the flow through a single feature i. The resulting internal flood height is computed considering the cumulative flow through all features using a converging structure. The flow through a flood protection feature can be quantified with high-fidelity simulations such as RAVEN [71], and Neutrino [72], or through physical relationships quantified with MC simulation as is the case in this study. In this study, the flow through a single feature is modeled as a function of random variables t_{E_i}, $\Delta\eta_{E_i}$, and A_i (i.e., the hydraulic head above the feature and its duration, as well as the cross-sectional area of the feature lost due to damage).

Specifically, this study models the flow volume, V_i, through a single damage feature is $V_i = t_{E_i} C_d \sqrt{2g(\Delta\eta_{E_i} - \eta_{ins_i})} A_i$, where C_d is the coefficient of discharge and g $(\frac{m}{s^2})$ is the gravitational constant. A_i is represented as a deterministic function of its parent node C_i, and η_{ins_i} is a deterministic value. In the formulation used herein, t_{E_i} is assumed to be either independent of

or as a stochastic function of flood level– thus it does not need to be explicitly included as a node in the BN and can be handled via the MC simulation.

Therefore, to reduce discretization error and computational memory demands, the purple dashed nodes in Figure 3 are represented through V_i, rather than explicitly modeled in the BN by considering physical relationship and use of MC simulation. Note that this study retains $\Delta\eta_{E_i}$ due to its relevance in modeling the flood protection feature state C_i and the possible need to enter observations related to that node. The use of the physical models to integrate out relevant random variables transforms the BN in Figure 3 to BN shown in Figure 6.

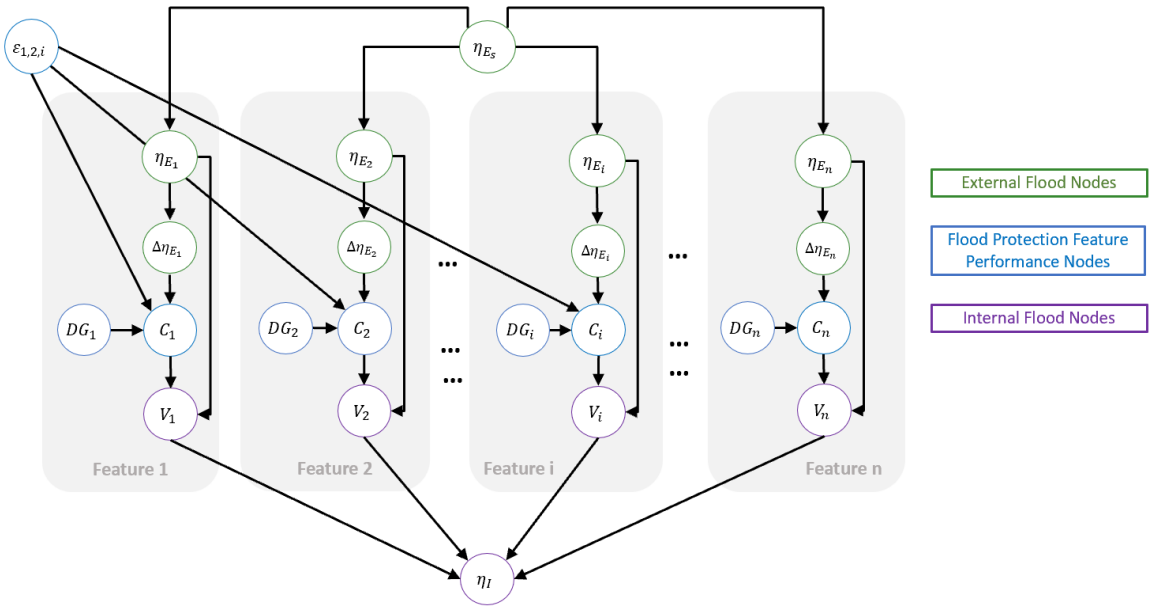

Figure 6:General MC-BN with Relevant Internal Flood Nodes Eliminated from the BN

3.3.8 Internal flood depth Node η_I

The internal flood depth node η_I, is a random variable that models the internal flood depth as a function of the final cumulative flow volume modeled in the BN. η_I is modeled as a depth to account for the changing internal floor elevation η_{floor}, as the floor can be below, at, or above plant-grade elevation and the elevation of η_{ins_i}. The internal flood depth node is a direct mapping of the sum of each flow volumeV_i and the internal room dimensions, with a cap to account for the physical configuration. For example, assuming that the flood protection feature is above floor elevation, the depth of water in the room may be calculated as $\min\left(\frac{\sum_{i=1}^{n} V_i}{A_r}, \left(\eta_{ins} - \eta_{floor}\right)\right)$, where A_r represents the floor area of the room.

3.4 Representative Case Study

Using an illustrative case study, this paper demonstrates the MC-BN approach presented in Section 3.3. Recognizing that all data in this context is site-specific, the case study applies demonstrative assumptions with justifications that are cited when applicable. The assumptions, flood protection features, and relevant variables in this case study were selected to produce meaningful results, but do not reflect the conditions of any site.

The generalized methods provided in Section 3.3 are applied to a building envelope with a single internal room on site with varying topography, as illustrated in Figure 7a. The site is

subjected to storm surges from the nearby body of water, measured from the reference datum of MSL. The plant is sited at an assumed elevation of 1.83 m MSL.

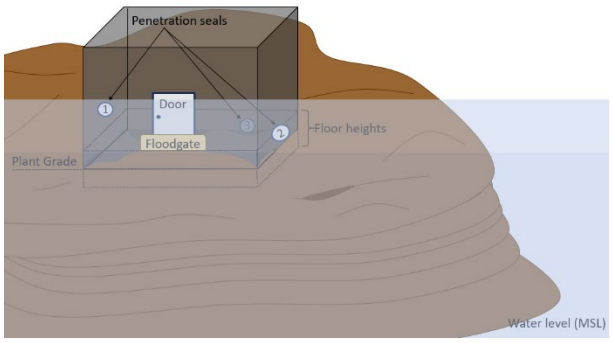

(a)

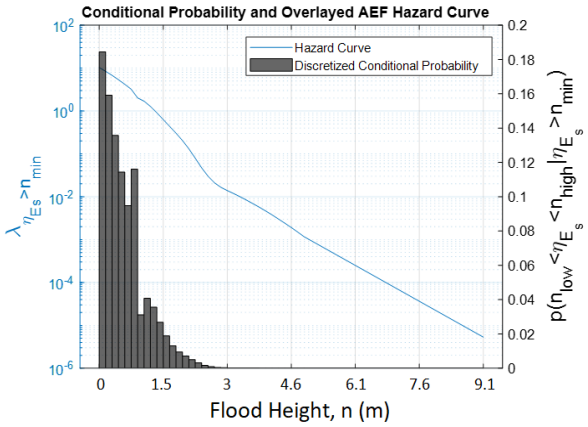

(b)

Flood Barrier	DG_i =Undegraded	DG_i =Degraded	DG_i =Failed
Conduit Penetration Seal	0.82	0.11	0.07
Pipe Penetration Seal	0.79	0.18	0.03
**Door	1	0	0

**Floodgate pre-existing degradation probabilities are assumed to be the same as the door

(c)

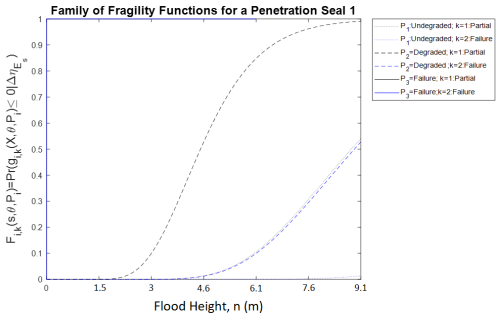

(d)

Figure 7: (a) Illustrative Building Site; (b) Hazard Curve and Discretized Conditional Probability of Hazard; (c) Flood Protection Features Pre-Existing Degradation States and Probabilities; (d) Family of Fragility Functions for Penetration Seal 1

The representative building envelope consists of five flood protection features: a floodgate protecting a door and three identical penetration seals on differing faces of the building and at varying elevations. Their assumed elevations and installation heights relative to plant grade are summarized in Table 2.

Table 2: Installation Height of Flood Protection Features

Flood protection feature	i	Elevation (m, MSL)	Installation height relative to nominal plant grade (m)
Penetration seal 1 (PS_1)	1	0.91	-0.91
Penetration seal 2 (PS_2)	2	1.8	0
Penetration seal 3 (PS_3)	3	2.7	0.91
Door (D)	4	1.8	0
Floodgate (FG)	5	1.8	0

Adapting the general BN from Figure 6 to the case study results in the BN shown in Figure 8. The floodgate and the door are co-located and, therefore, share the same external hazard, and the associated flow through the door opening depends on the performance of both the gate and the door. The general methods presented in Section 3.3 are applied to each node.

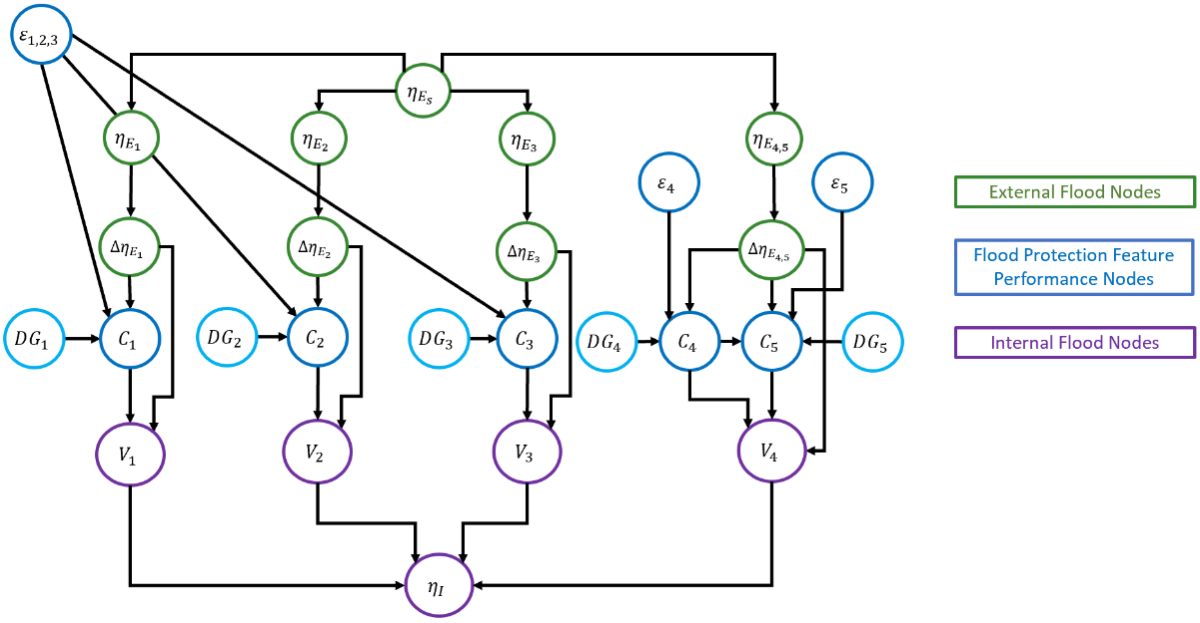

Figure 8: Proposed BN Applied to Representative Site

For brevity, the methods provided in Sections 3.5 – 3.10 are applied to nodes relevant to the first penetration seal. Therefore, unless explicitly required for relevant discussion, all subsequent values provided for demonstrative purposes are in the context of penetration seal 1.

3.5 External Flood Elevation Node η_{E_s}, Feature Specific Elevation Node η_{E_i}, and Flood Demand $\Delta\eta_{E_i}$

Applying the method in Section 3.3.1, this study leverages a hazard curve from the U.S. Army Corps of Engineers' (USACE) North Atlantic Coast Comprehensive Study (NACCS) [73] at a representative site to generate the CPT for η_{E_s}. The hazard curve is extrapolated to a flood

elevation of zero meters, MSL. The AEF is discretized to generate conditional probabilities of $P_{\eta_{E_S}}\left(n_{low} \leq \eta_{E_S} < n_{high} \middle| \eta_{E_S} > \eta_{min}\right)$ to become an input for the η_{E_S} CPT by adapting work from Baker [74]. The bins are defined by bin edges n_{low} and n_{high}, given η_E exceeds a threshold elevation η_{min}, which is assumed to be zero meters MSL. This study discretizes the external flood site elevation hazard curve into bin widths of 0.15 m from zero to 4.5 m and above, resulting in 31 states. Figure 7b plots the extrapolated hazard curve in blue against the left y-axis. The discretized conditional probability (used to define the marginal probability table of node η_E) is plotted in black against the right y-axis. This case study site has no topographic characteristics between the building and the flood source. Therefore, the site-specific flood elevations $\eta_{E_i}, i = 1, \ldots, 5$ are equivalent to its parent node η_{E_S} (i.e., the CPT is an identity matrix).

External flood elevation is transformed into a demand by accounting for η_{ins_i}. Therefore, the CPTs are a direct mapping based on these relationships. Flood demand has a similar discretization as its parent node with the addition of a "no flood" state of zero meters, resulting in 32 total states. If the discretization differed, the MC simulation approach described in Section 3.3.7 can be used to account for differences between states. The number of entries in the CPT assigned to a node is defined by the combination of states of the node and its parent node(s). Therefore, for the $\Delta\eta_{E_1}$ CPT, there are ($32 * 31 = 992$ entries).

3.6 Pre-Existing Degradation Nodes DG_i

Pre-existing degradation DG_i is defined in Section 3.3.3 and describes the degradation incurred before the flooding event. This paper assumes each flood protection feature has three possible pre-existing degradation states: undegraded, degraded, and failed (the floodgate and door similarly have three pre-existing degradation states: Installed-Perfect, Installed-Degraded, and Not Installed). These states are defined by leveraging the in-depth review of flooding walkdown reports by Ma et al. [69]. These pre-existing degradation probabilities for various flood protection features from the report are provided in Figure 7c. Pre-existing degradation probabilities for the floodgate are assumed to be the same as the door, as floodgates are not explicitly provided in the literature. The pre-existing degradation can have a physically deteriorating effect on the flood protection feature's capacity. As seen in Equation 3, pre-existing degradation is accounted for in the median capacity through an *apriori* assumed reduction factor $P_{i,k} = [0, 0.5, 0.99]$ for undegraded, degraded, and failed states and, therefore, have 3 states. In this study, the degradation states are assumed to be independent, but dependence could be included in the BN, for example, by using a strategy like that used for modeling fragility correlation.

3.7 Flood Protection Feature State Nodes C_i

Feature state probabilities are quantified through an MC simulation using the limit state function outlined in Section 3.3.4. There is limited literature on flood protection feature capacities

against flood demands. Therefore, this case study leverages the high-confidence-low-probability-of-failure (HCLPF) capacity to generate the flood protection feature's best-estimate capacities.

3.7.1 Median Capacity Calculation Leveraging High-Confidence-Low-Probability-of-Failure Capacities

The HCLPF approach has been extensively used in conjunction with seismic PRAs [75] [76] and is modified herein to support external flooding PRA. The HCLPF capacity is a perceived demand that has a high confidence that there is a low probability of reaching or exceeding a damage state k. Assuming capacity is modeled as a lognormal random variable, the relationship between the median and HCLPF capacities is given by:

$$\Theta_{HCLPF} = \Theta_{med,i,k} \exp\left(\Phi^{-1}(p) \times \zeta_{comp}\right) \qquad \text{Equation 4}$$

where Θ_{HCLPF} is the HCLPF capacity, $\Theta_{med,i,k}$ is the lognormal median capacity, and $\Phi^{-1}(p)$ is the inverse standard normal cumulative distribution function at a selected failure probability p. In seismic applications, the low probability of failure p is taken at $p = 0.05$ of the 95% confidence fragility curve to capture this high confidence [75]. This value is approximately equivalent to $p = 0.01$ on the median fragility curve, which is the value at which the HCLPF is determined. This study assumes the lognormal composite standard deviation ζ_{comp} is 0.3, which is obtained from a representative range ($0.3 \leq \zeta_{comp} \leq 0.6$), provided by the American Society of Civil Engineers

(ASCE) standard “Seismic Design Criteria for Structures, Systems and Components in Nuclear Facilities.” [77]

The HCLPF capacities used in this case study are sourced from a literature survey, which assumes that the technical specification head rating corresponds to the HCLPF value. This assumption is considered reasonable to support this case study, but additional research is needed to confirm this relationship. Penetration seal HCLPF capacities were specifically synthesized from manufacturer technical specifications [78] [79] [80] [81]. Door HCLPFs were sourced from experiments by Pope et al. [46], and floodgates were assumed to fail when overtopped by the flood depth. Leveraging Equation 4 with representative HCLPF capacities from the literature survey, this study assumes two damage states of partial damage and complete failure, generating the respective undegraded median capacities to resist hydraulic head. In the case of penetration seals, the median capacities for partial and complete failure are 8.8 m and 18 m. $R_{i,k}$ is a reduction factor on the median capacity used to increase the probability of reaching or exceeding a given damage state for a specified demand, and is associated with a pre-existing degradation state: pre-existing degradation states: undegraded, degraded, and failed with respective reduction factors $R_{i,k} = [0.99, 0.5, 0]$. While the capacity uncertainty does not vary with degradation in this case study, the proposed model can be adapted to include this consideration.

3.7.2 Monte Carlo Approach for Obtaining C_i CPTs

As shown in Figure 8, the flood protection feature state is a child node to flood demand, pre-existing degradation, and fragility error. Specifically, this study emphasizes the effect of pre-existing degradation on the capacity. The limit state function, as provided in Equation 1, and capacity term, provided in Equation 3 can be logarithmically transformed to the form in Equation 5. The log transformation of the limit state function can separate the median capacity and fragility terms, resulting in $\ln(CAP_{i,k}) = \ln(\Theta_{med,i,k} * R_{i,k}) + \ln(E_R) + \ln(E_U)$. Furthermore, this study simplifies capacity by combining the aleatory and epistemic uncertainty variables into a single term, $\varepsilon_i = \ln(E_R) + \ln(E_U)$.

$$g^*_{i,k}\left(\varepsilon_i, \Delta\eta_{E_i}\right) = \ln(\Theta_{med,i,k} * R_{i,k}) + \varepsilon_i - \ln\left(\Delta\eta_{E_i}\right) \leq 0 \qquad \text{Equation 5}$$

Where $g^*_{i,k}\left(\varepsilon_i, \Delta\eta_{E_i}\right)$ is the log transformation of Equation 1, using capacity as depicted in Equation 1. This study uses MC simulation to generate the conditional probability of the feature being in each damage state as a function of the parent nodes by sampling from each discrete bin of ε_i and $\Delta\eta_{E_i}$ (see note[8]) and computing the fraction of samples for which the limit state function indicates failure. The number of CPT entries is the combination of the number of states of C_1 and

[8] For the discrete ε_i state $\{\varepsilon_{low} \leq \varepsilon_i < \varepsilon_{high}\}$, N_{sim} MC simulation samples are drawn from a normal distribution truncated on the domain $[\varepsilon_{low}, \varepsilon_{high}]$ (see Section 3.3.5 for a description of the distribution of ε_i). For the discrete $\Delta\eta_{E_i}$ state $\{\Delta\eta_{E_{low}} \leq \Delta\eta_{E_i} < \Delta\eta_{high}$, N_{sim} MC simulation samples are drawn from a uniform distribution on the domain $[\Delta\eta_{E_{low}}, \Delta\eta_{high}]$.

its parent nodes DG_1, ε_1, and $\Delta\eta_{E_1}$ $(3 \cdot 3 \cdot 15 \cdot 32)$, resulting in a total of 4,320 entries. A snippet of the CPT is provided below:

Table 3: Snippet of C_{PS_1} Node CPT

C_1	…	$\Delta\eta_{E_1} = 4.6$ and above (m)			
	…	$\varepsilon_{1,2,3} = -0.54$ to -0.42			…
	…	DG_1 = Undegraded	DG_1= Degraded	DG_1 = Failed	…
$k = 0$	…	0.62	0	0	…
$k = 1$	…	0.38	0.665	0	…
$k = 2$	…	0	0.335	1	…

3.8 Fragility Error Nodes ε_i

This study assumes fragility error is normally distributed with a mean of zero and a standard deviation of 0.3, consistent with ζ_{comp}. For the case study, the fragility error states are obtained by discretizing the domain of ε_i within approximately $\pm 3\sigma_\varepsilon$ and using an odd number of bins to ensure the distribution is centered about zero. The probability within each bin is obtained directly using the standard normal cumulative distribution function $\Phi(\cdot)$; i.e., $P(\varepsilon_{low} \leq \varepsilon_i < \varepsilon_{high}) = \Phi\left(\frac{\varepsilon_{high}}{\sigma_\varepsilon}\right) - \Phi\left(\frac{\varepsilon_{low}}{\sigma_\varepsilon}\right)$. The lowest and highest bin edges are replaced with $-\infty$ and $+\infty$ to ensure the entire domain of the normal distribution is captured.

The domain of $\varepsilon_{1,2,3}$ is discretized into 15 bins, resulting in 15 entries for the fragility error CPT. A snippet of the CPT of the fragility error for penetration seals is provided below.

Table 4: Snippet of $\varepsilon_{1,2,3}$ Node CPT

$\varepsilon_{1,2,3}$	
$-0.9\ (-\infty)\ to\ -0.78$	0.005
$-0.78\ to\ -0.66$	0.009
$-0.66\ to\ -0.54$	0.022
$-0.54\ to\ -0.42$	0.045
…	…

3.9 Flow Volume Nodes V_i

As discussed in Section 3.3.7, flow volume through a penetration is modeled as V_i, as adapted from the Bernoulli equation, $V_i = t_{E_i} C_d \sqrt{2g(\Delta\eta_{E_i} - \eta_{ins_i})} A_i$. These functions are quantified with MC simulation, arbitrarily assuming $t_{E_i} \sim NORM(\mu = 3600\ s, \sigma = 0.2 * \mu)$ and $A_i \sim NORM(\mu_k, \sigma = 0.2 * \mu_k)$ where μ_k is associated with each damage state. Given assumed parameters, MC simulation is used to define the conditional PMF of V_i for all combinations of its parent nodes, C_i, and $\Delta\eta_{E_i}$,[9] yielding a CPT with $(22 \cdot 3 \cdot 32) = 2{,}112$ entries. Note that the states of Vol_i are defined through increments of 5% of the total room volume, V_r. A snippet of the CPT for V_1 is provided below.

[9] N_{sim} MC simulation samples of t_{E_i} are drawn from the specified normal distribution. For the discrete $\Delta\eta_{E_i}$ state $\{\Delta\eta_{E_{low}} \leq \Delta\eta_{E_i} < \Delta\eta_{high}$, N_{sim} MC simulation samples are drawn from a uniform distribution on the domain $[\Delta\eta_{E_{low}}, \Delta\eta_{high}]$. For each state of C_i, N_{sim} MC simulation samples of A_i are drawn from the specified normal distribution.

Table 5: Snippet of V_1 Node CPT

V_1 (m^3)	$\Delta\eta_{E_1} = 0$ to 0.5 (m)						…
	$k = 0$			$k = 1$			…
$0 * V_r$	0	0	0	0	0	0	…
$(0\ to\ 0.05) * V_r$	1	0.906	0.417	1	0.393	0.018	
$(0.05\ to\ 0.10) * V_r$	0	0.094	0.544	0	0.595	0.459	
$(0.10\ to\ 0.15) * V_r$	0	0	0.039	0	0.012	0.480	…
…	…	…	…	…	…	…	…

3.10 Internal flood depth Node η_I

As discussed in Section 3.3.8, internal flood depth is a direct mapping of the sum of all flow volumes V_i. The internal room floor area, taken as a representative value of $A_r = 58$ m^2, is used to convert the volume to internal flood depth. The internal flood depth is limited by the resulting internal flood depth given all previous variables, and the height of the roof relative to the floor, depending on whether the floor is below, at, or above plant grade. This study assumes an internal room height of $n_r = 3.05$ m with the floor elevation at plant grade. The number of entries is determined by the state combinations of η_I and its parent nodes $V_{i=1,2,\dots n}$ $(22 \cdot 22 \cdot 22 \cdot 22 \cdot 22)$ resulting in 5,153,632 entries.

3.11 Bayesian Inference

As discussed in Section 3.1, BNs can facilitate multi-directional inference by enabling the analyst to enter evidence on a node(s) in the BN. Observed states for a specified node(s) can propagate through the network, updating the other nodes' distributions. This allows analysts to identify likely states of variables within the system, increasing model transparency and yielding

additional insights. This study uses a few evidence case studies to demonstrate forward and backward propagation and highlight system response and vulnerabilities that can be gleaned from the Bayesian updating.

3.11.1 Demonstrative Case Study: Forward Propagation

To illustrate the predictive capabilities of BNs, this study considers a series of forward propagation evidence cases (ECFs), set on the three penetration seals, as shown in Figure 9. As these ECFs are propagated forward, the BN allows practitioners to understand its impact on all subsequent children nodes. As well as preceding parents, ECF0 is the no-evidence case, whereas ECF1, ECF2, and ECF3 are associated with the occurrence of an elevation associated with a 50-year, 100-year, and 500-year flood, at a given site respectively. ECF4, ECF5, ECF6, and ECF7 augment ECF0-ECF3 by considering degraded penetration seals, which can provide further insights into the joint effects of a flood and pre-existing degradation states. ECF8, ECF9, ECF10, and ECF11 instead consider the penetration seals in a failed pre-existing state. The right column of Figure 9 shows the effect of the evidence cases on the probability mass function (PMF) of the internal flood height node.

ECF0-ECF3 show how entering evidence of an increasing external flood elevation shifts the posterior internal flood depth distribution to the right, which aligns with the case study assumptions. The next set of ECFs considers each penetration seal being in the degraded (ECF4-ECF7) or failed (ECF8-ECF11) pre-existing states. ECF4-ECF7 highlights that degraded

penetration seals do not have a significant impact on the resulting internal flood depth. This suggests that, given the assumptions of the case study, pre-existing degradation may not impact the performance of the flood seals in a meaningful way, or the degradation probability (before entering evidence) is sufficiently high that the entering of evidence does not have a substantial quantitative effect. However, when the penetration seals have a pre-existing failure, as seen in Figure 9(c) for ECF8-ECF11, there is a greater impact on internal flood distribution, shifting towards larger internal flood heights.

The internal flood distributions are bimodal, as seen in each graph of Figure 9. This is due to the selected evidence cases, which all have the potential to produce flood depths above the floodgate's height. Flood depths above the floodgate's height result in complete failure due to overtopping, triggering large internal flood depths, as well as the large flow area through the door, resulting in the second peak at higher internal flood depths of 2.9 m or greater.

ECF	Description	PMF of Internal Flood Depth given ECF
0	No evidence related to flood	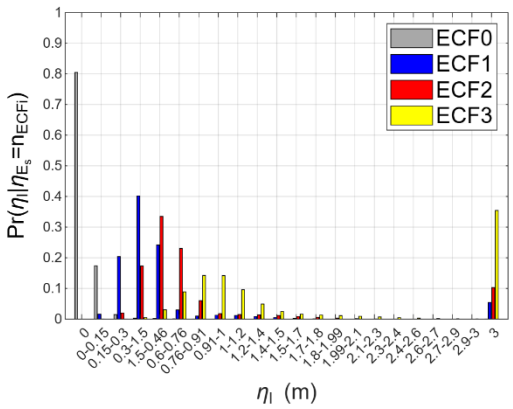 *(a)*
1	50-yr flood: $\eta_{E_S} = 2.7$ m	
2	100-yr flood: $\eta_{E_S} = 3.4$ m	
3	500-yr flood: $\eta_{E_S} = 4.4$ m	
4	EC0 + degraded penetration seals	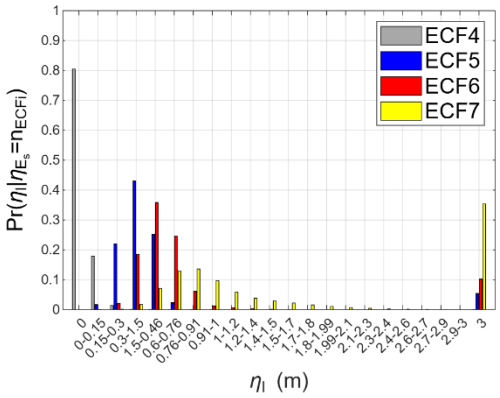 *(b)*
5	ECF1 + degraded penetration seals	
6	ECF2 + degraded penetration seals	
7	ECF3 + degraded penetration seals	
8	ECF0 + failed penetration seals	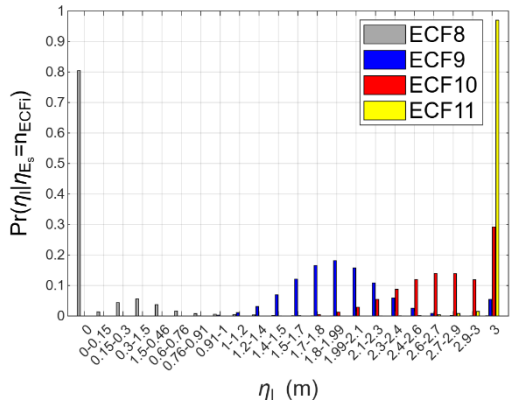 *(c)*
9	ECF1 + failed penetration seals	
10	ECF2 + failed penetration seals	
11	ECF3 + failed penetration seals	

Figure 9: Forward Inference of (a) ECF0-3 (b) EC4-7 (c) ECF8-11 to Internal Flood Depth

3.11.2 Demonstrative Case Study: Backward Propagation

Evidence can also be propagated backwards to diagnose system states. The diagnostic capabilities of the BN are demonstrated by propagating evidence on the internal flood depth to pre-existing degradation states for flood protection features. Backward propagation in the BN provides insights of likely configurations of parent nodes given observations related to child node states. This example considers three backwards propagation evidence cases (ECB), in which the internal flood depth η_I is assumed to be 0 m (ECB1), 0.61 m (ECB2), and 3 m (ECB3). These internal flood depths were selected to demonstrate no flood, a moderately flooded room to capture partial submergence of safety SSCs, and a fully flooded room scenario. These evidence cases are backwards propagated to the pre-existing degradation node of penetration seal 1 (Figure 10(a)), the floodgate (Figure 10(b)) and the door (Figure 10(c)), comparing each distribution to the no evidence cases (ECB0).

In line with the model's assumptions, the no evidence case and internal flood depth of zero m have nearly the same distributions because zero m is the likeliest internal flood depth. A meaningful insight gleaned for penetration seals is that the probability of pre-existing degradation, given no flood and a severe flood, has similar values. An observed moderate flood leads to a higher likelihood of the penetration seal being in a failed pre-existing state. This indicates that, given a severe flood, other flood protection features are more impactful in contribution, which is the case

for the comparatively higher likelihood of a pre-existing failed state of the door. This follows the large flow area assumption associated with the failed degradation states of the door.

The floodgate's pre-existing distributions are fairly consistent regardless of the internal flood depth evidence cases. This consistency indicates that the damage to the floodgate and other features is from the flood demand rather than the pre-existing state. There is a larger contribution to the failed pre-existing state of the door. This is likely due to the configuration that the door is the final flood protection feature with the largest flow area.

ECB	Flood Protection Feature	Evidence State	PMF of Pre-Existing Degradation for flood protection feature i given ECB
0	Penetration Seal 1	No evidence	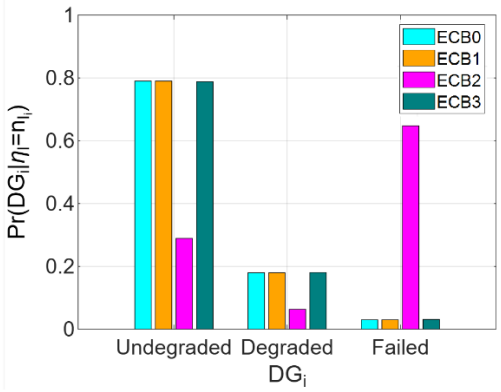 *(a)*
1		$\eta_I = 0$ m	
2		$\eta_I = 0.61$ m	
3		$\eta_I = 3$ m	
0	Floodgate	No evidence	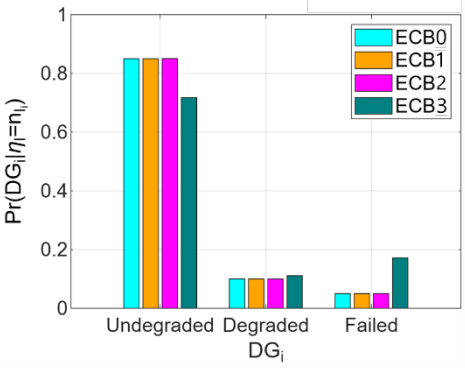 *(b)*
1		$\eta_I = 0$ m	
2		$\eta_I = 0.61$ m	
3		$\eta_I = 3$ m	
0	Door	No evidence	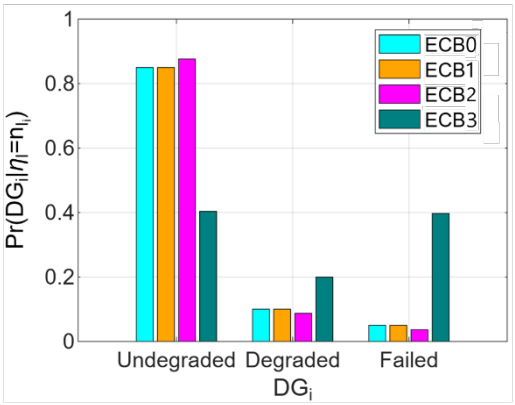 *(c)*
1		$\eta_I = 0$ m	
2		$\eta_I = 0.61$ m	
3		$\eta_I = 3$ m	

Figure 10: Backward Inference ofη_I to (a) Penetration Seal, (b) Floodgate, and (c) Door

3.12 Summary and Conclusion

This study proposes a BN as a tool to probabilistically model an external flood impacting an NPP site. The study expands external flood PRA modeling capabilities by leveraging an MC-BN as an alternative risk tool. BNs are appropriate for incorporating Bayesian updating, improving SSC and temporal dependency modeling, and addressing spatial variability and the binary component state assumption. Specifically, this study creates an MC-BN, tracking an external flood event from the flood initiator to the internal flood depth by considering the impact on feature performance. The BN provides a transparent and traceable model while preserving the model's robustness in representing the external flood event. The static external flood impacts the site, assuming the bath-tub propagation with a spatial variability assumption in the site, expressed in nodes modeling elevation, depth, and duration. The flood affects feature performance, considering correlated fragility error, pre-existing degradation, and component damage state. Given the performance of the features, the flood may infiltrate critical areas expressed as a flood volume and internal flood depth inside a room. The MC Simulation is leveraged to reduce computational demand, simplify the BN structure, and quantify the functions of random variables. The MC Simulation provided in this study uses analytical relationships in a closed form. These simplified models may be replaced by more sophisticated models, such as high-fidelity numerical simulations. Furthermore, most data and experience are based on the binary structure of the conventional tools, which have difficulties when transitioning to a multi-state structure.

A case study is applied to illustrate the capabilities of the MC-BN approach. Using judgment-based assumptions, the results provide insights by enabling predictive and diagnostic inference. The results from the case study underlined the usefulness of leveraging a BN in making risk-informed decisions and identifying vulnerabilities that may be masked by challenges associated with conventional risk tools. The MC-BN approach provides a framework to transparently track external flood modeling. The BN is expanded to incorporate equipment performance under flood conditions, leveraging advantages in conventional and alternative risk tools to form a hybrid framework.

Chapter 4. A Hybrid External Flood Probabilistic Risk Assessment Framework Leveraging a Monte Carlo Augmented Bayesian Network

4.1 Hybrid External Flood Probabilistic Risk Assessment Configurations

To showcase the full extent of how an MC-BN can improve on the flood modeling and assumptions in ETs and FTs, we present a spectrum of relevant configurations that illustrate strategies for integrating BN-derived information in the PRA. In this context, the PRA evaluates the external flood hazard as the initiator, including flood-induced and random failures, resulting in unsafe outcomes.

To illustrate the capabilities of the MC-BN, ETs and FTs, four logically and quantitatively equivalent hybrid configurations are considered: (1) MC-BN approach, (2) ET/FT approach using MC-BN Derived Probabilities, (3) External Flood MC-BN Approach, and (4) Hybrid Causal Logic Approach. Each configuration was verified through intermediate and final probability distributions to be equivalent to allow a direct comparison of the advantages and limitations of each application.

To generate equivalent models, Configuration 1 serves as the basis of all other configurations' logic and probabilities. Hybrid configurations with a BN portion are directly copied from Configuration 1, whereas ETs and FTs are simplifications of the BN logic and probabilities by reducing multiple states to binary (consistent with the limitations of the ET/FT

framework) for all nodes that provide input to the ET/FT. Probabilities required by the ET/FT are obtained from the BN by marginalizing across multiple variables.

- **Configuration 1 – MC-BN Approach (Section 4.1.1)**: This configuration performs the PRA entirely within the MC-BN. All calculations are performed in either the MC simulation or the BN structure.
- **Configuration 2 – ET/FT Approach Using MC-BN-Derived Probabilities (Section 4.1.2)**: This configuration performs the PRA entirely within ETs and FTs.
- **Configuration 3 – External flood MC-BN hybrid approach (Section 4.1.3)**: This configuration delegates the flood modeling to the MC-BN, in which the external and internal flood effects are modeled. This results in a discrete internal flood probability distribution that is used as an input for a top event in an ET with multiple branches.
- **Configuration 4 - Hybrid Causal Logic Approach (Section 4.1.4)**: This configuration implements the hybrid causal logic approach [54] [55] [56]. It delegates the external flood model and its effects on safety-related SSCs to the BN. The resulting flood fragility of the safety-related SSCs is used as a basic event probability in the associated safety-equipment FT.

4.1.1 Configuration 1: Monte Carlo Augmented Bayesian Network Approach

The MC-BN serves as the baseline model and is shown in Figure 11, with the variables represented in the nodes (circles) and the conditional relationships indicated by the links (arrows). Node definitions are provided in Table 6. Relationships reflected in a BN are described in familial terms, where the parent node is the variable that influences another node known as the child node. The BNs in this work have a black dot to indicate the parent node, and the arrow points to the child node.

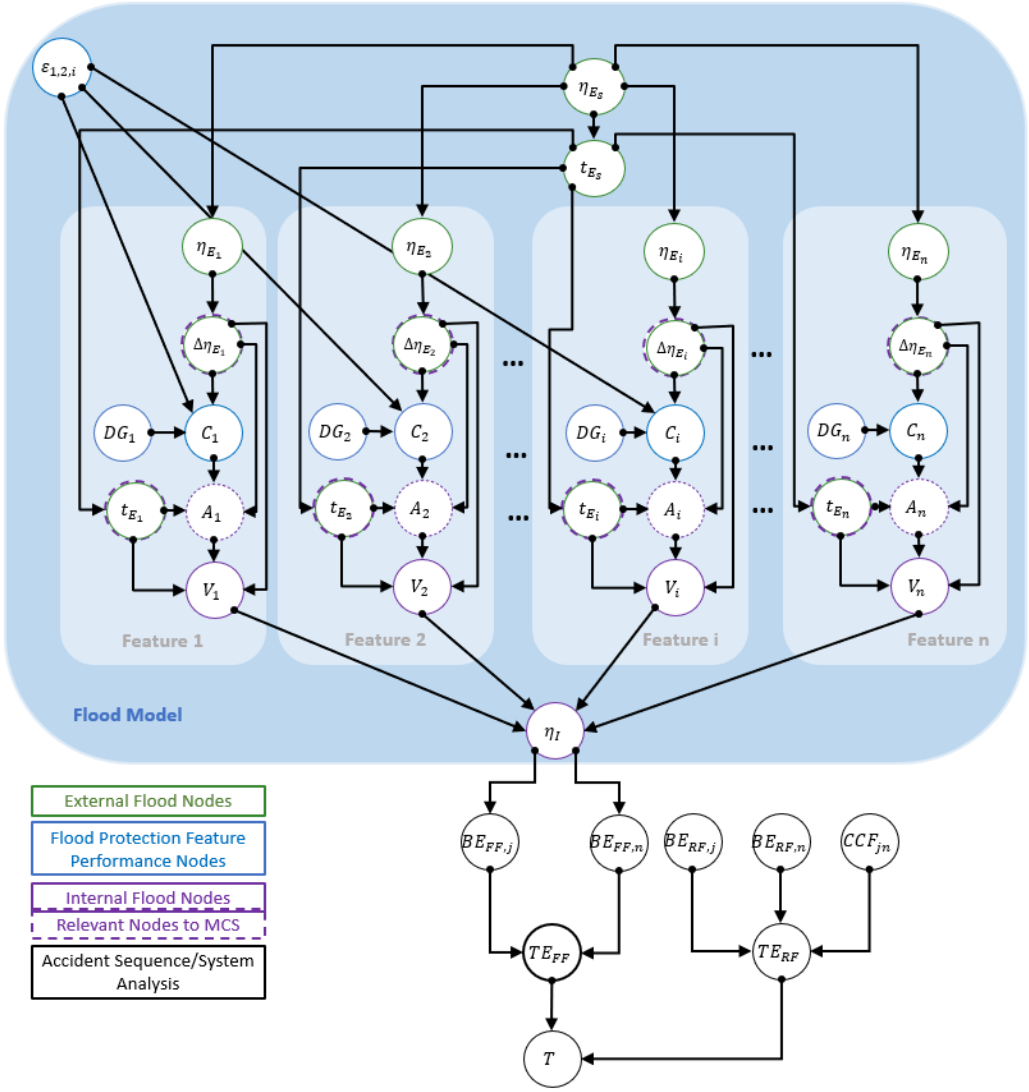

Figure 11: External Flood BN

The MC-BN model, described in Shen et al. [1] , models an external flood impacting an NPP site. The BN's logic begins by characterizing the external flood as represented by the green nodes in Figure 11. The reference external flood elevation and associated flood duration (conceptually analogous to the concept of a control point hazard commonly used in conjunction with seismic

hazards [83]) are represented by nodes η_{E_S} and t_{E_S}, respectively. The flood is propagated across the site, impacted by the site's characteristics and structural flood protection features such as seawalls, resulting in an elevation η_{E_i} and flood duration t_{E_i} at the location of flood protection feature i. The flood demand on the feature is then modeled as the flood depth $\Delta\eta_{E_i}$, which is calculated from the feature's installation height to the flood elevation.

The nodes in blue represent the performance of the flood protection features, which consists of the feature's performance given the flood demand, C_i, which has influence from pre-existing degradation DG_i. Once the flood has passed through the degraded and/or damaged feature, the internal flood nodes in purple represent the flood that is infiltrating the building. To reduce memory and computational demands, an MC simulation integrates flow area and flood duration through physical relationships. The internal flood η_I is measured from the floor of the internal building, which may be below, above, or at plant grade.

The infiltration of floodwater into buildings that house safety-related SSCs can affect a plant's ability to safely operate or shut down, represented by the flood-induced flood failure node, TE_{FF}, which is a child node of η_I to model SSC failures given the flood depth impacting the SSC. Additionally, the SSC can become inoperable by random failure, represented in the root node

TE_{RF}. Both TE_{FF} and TE_{RF} are labeled in black nodes in Figure 11.[10] Flood-induced failures model the effects of floodwaters on mechanical and electrical SSCs (e.g., short-circuiting, fuel contamination, etc.) while random failures model the resultant failure phenomenon (e.g., failure to start, failure to run, failure to operate, etc.). Both can be decomposed into basic events induced by the flood (BE_{FF}) or induced randomly (BE_{RF}), where the TE_{RF} also models CCF between identical components j and n (CCF_{jn}). Thus, transient T that can be flood-induced, random, or a combination of both, and are referred to as accident sequence and system analysis nodes outlined in black. These nodes shown in Figure 11 are summarized in Table 6. V_i is differentiated by an asterisk ($*$) to indicate that it contains relevant internal flood nodes that were integrated out by an MC simulation.

[10] The notation "TE" in the node labeling convention reflects that these events are typically represented as "top events" in conventional ET models.

Table 6: Nodes and Node Category Descriptions

Node Group	Random Variable	Description
External flood nodes	η_{E_s}	Flood elevation at the site reference location with respect to a reference datum
	$\eta_{E\,i}$	Flood elevation at the location of flood protection feature $i = 1,2, \dots, n$
	$\Delta\eta_{E_i}$	Flood demand on flood protection feature $i = 1,2, \dots, n$
Flood Protection Feature Performance Nodes	DG_i	Pre-existing degradation state of flood protection feature $i = 1,2, \dots, n$
	ε_i	Fragility error associated with component $i = 1,2, \dots, n$
	C_i	State of flood protection feature $i = 1,2, \dots, n$
Internal Flood Nodes	A_i	Cross-sectional area of flood protection features $i = 1,2, \dots, n$ lost due to damage
	V_i*	Flow volume through flood protection feature $i = 1,2, \dots, n$
	η_I	Internal flood depth within the structure
External Flood Plant Response	IE	Initiating event of the accident sequence
	TE_{FF}	Top event modeling a flood failure state
	TE_{RF}	Top event modeling random failure
	$BE_{FF,j}$	Basic event representing a flood failure of SSC $j = 1,2, \dots n$
	$BE_{RF,j}$	Basic event representing a random failure of SSC $j = 1,2, \dots n$
	T	Transient

4.1.2 Configuration 2: ET/FT Approach Using MC-BN-Derived Probabilities

Configuration 2 translates Configuration 1 to ETs/FTs, in which flood and random failures are modeled in conventional tools, as seen in Figure 12. However, this conversion of the BN to ET/FT logic is not a one-to-one mapping, as static ETs and FTs do not typically model spatial and temporal dependencies or multiple states for failures or fragility errors like BNs can. Therefore, this conversion is more accurately described as a quantitatively equivalent but simplified version of the BN's logic and probabilities. Specifically, because multiple states are not conventionally represented in ETs and FTs, the states of nodes in the BN that will provide input to the ET/FT are

discretized to be binary (e.g., by combining moderate and severe damage states into a failure state). Nodes that are not explicitly represented in the ET/FT are not modified but marginalized and represented in the selected child node's conditional probability. The probabilities assigned to each binary state are obtained by summing root notes or by marginalizing across the BN with forward inference such that the combined state reflects a weighted average of all previous node states. The use of forward inference in this manner ensures that the "simplified BN" provides quantitatively equivalent information (though the loss of discretization reduces the utility of using the BN).

Given these simplifying strategies, there are four relevant sets of ETs as seen in Figure 12:

a. External flood elevation ET
b. Flood protection feature's performance ET
c. Internal flood depth ET
d. External flood plant response ET

The external flood elevation ET begins with an initiating event frequency IE, which leads to initiator bins of the external flood elevation, η_{E_S}. This elevation ET transfers to the flood protection feature performance ET, modeling each unique sequence of feature states in C_i given an elevation of η_{E_S}. Each ET begins with a transfer initiating event, $IE - Transfer$ and models all possible features that are affected by the elevation of a given height. For each sequence of C_i, there is a resulting η_I distribution, represented in the following ET. This transfers into the final ET represents

the impact of each internal flood height on inducing flood and random failure of safety-related SSCs TE_{FF} and TE_{RF}. The ET that transfers into the sequential ET is indicated by the same color as the previous ET's top event. For example, the IE-transfer for Figure 12(b) is green as it is transferred from Figure 12(a)'s η_{E_s} initiator bin frequencies.

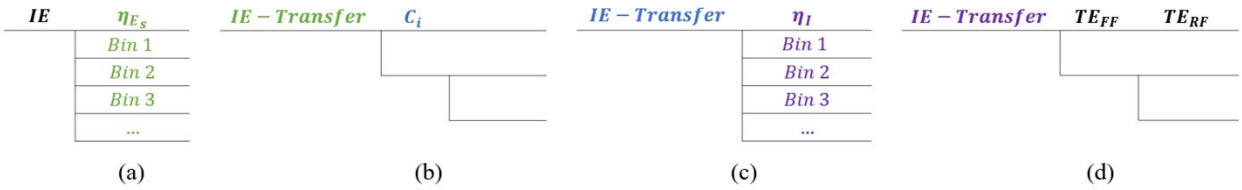

Figure 12: Conventional PRA Model

4.1.3 Configuration 3: External Flood MC-BN Hybrid Approach

As seen in Figure 13, the external flood MC-BN hybrid approach delegates the external flood modeling to the MC-BN, leveraging the BN developed in Configuration 1 from η_{E_s} to η_I. The conditional probability distribution of η_I is a weighted average, marginalized across all previous nodes' probabilities and uncertainties. The distribution is strategically integrated into the ET and FT, which in regard to the ET/FT approach in configuration 2, consists of Figure 12(a), Figure 12(c), and Figure 12(d). Specifically, the states and probabilities of the flood protection feature performance in Figure 12(b) are represented in the internal flood depth distribution. Note that the probabilities of the external flood elevation ET are also sourced from the η_{E_s} node from the BN. The dashed arrow from the node η_I in the BN to the top event η_I in the ET is to indicate where the

models are integrated between models. From this point, the ET models the accident sequence the same as external flood plant response ET in Figure 12(c) from configuration 2.

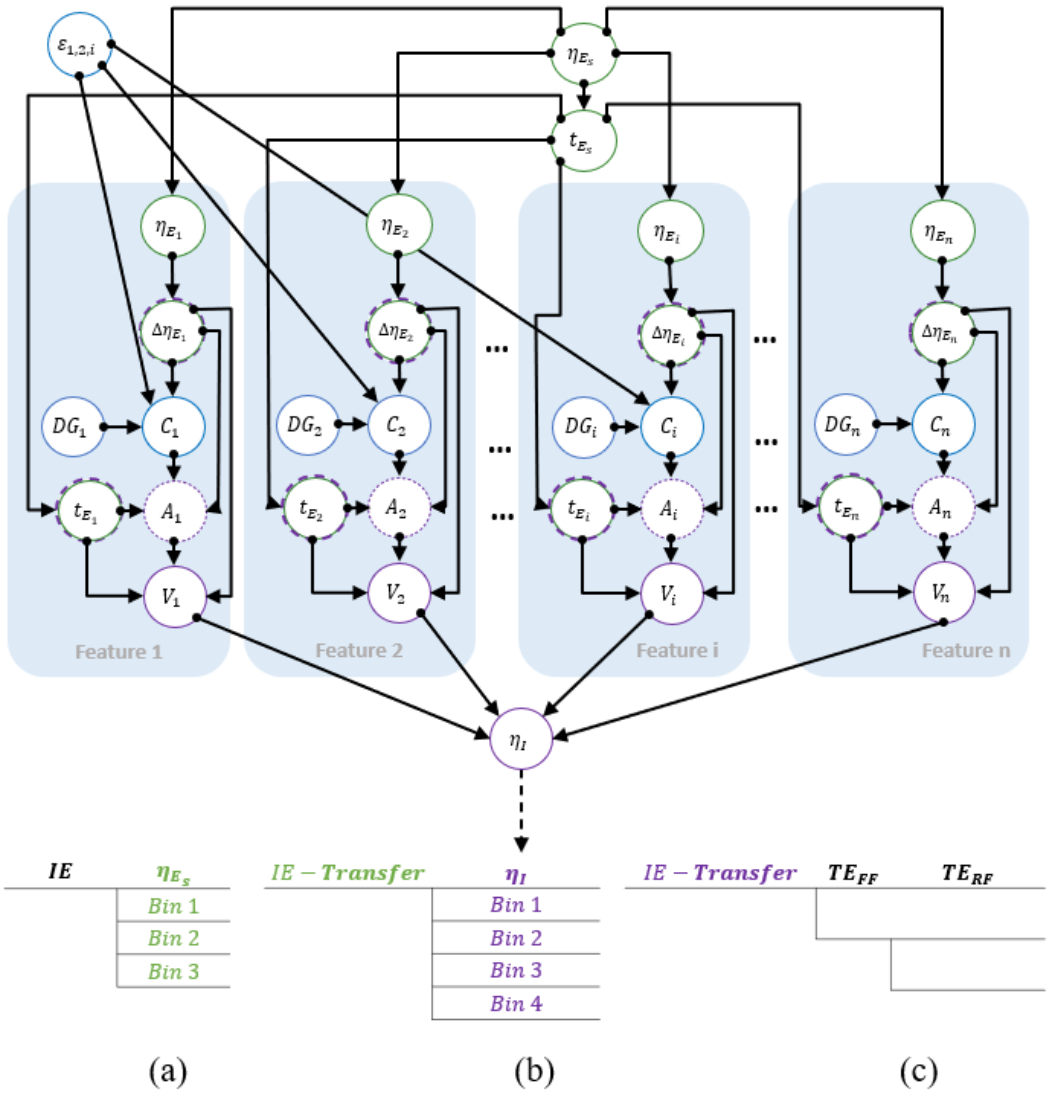

Figure 13: External to Internal Flood Configuration

4.1.4 Configuration 4: Hybrid Causal Logic Approach

Configuration 4 is the hybrid causal logic approach, [54], [82], [84] as seen in Figure 14. It delegates the external flood and the resulting flood fragility of safety-related SSCs in the MC-BN. However, Configuration 4 condenses TE_{FF} and TE_{RF} into $TE_{RF,FF}$ as the flood failure will be modeled alongside the random failures as a basic event. The BN as seen in Figure 14(d), is leveraged from η_{E_S} to TE_{FF}, generating the average weighted probability of safety-related SSCs flood failures. The BN is simplified to better illustrate the overall hybrid causal logic, which is indicated by the four rounded rectangles that represent each section of the BN modeling the external flood impacting each flood protection feature. Modeled alongside random failure basic events BE_{RF}, which lead to the flood and random induced failures of $SSC_{FF,RF,A}$ and $SSC_{FF,RF,B}$ with CCF. This resulting probability is binary to serve as an input as a BE_{FF} in the $TE_{FF,RF}$ fault tree in Figure 14(c), which has demonstrative logic and does not represent a specific system. This provides the top event probability for $TE_{FF,RF}$ in the external flood plant response ET in Figure 14(b), which is transferred from the external flood elevation ET Figure 14(a).

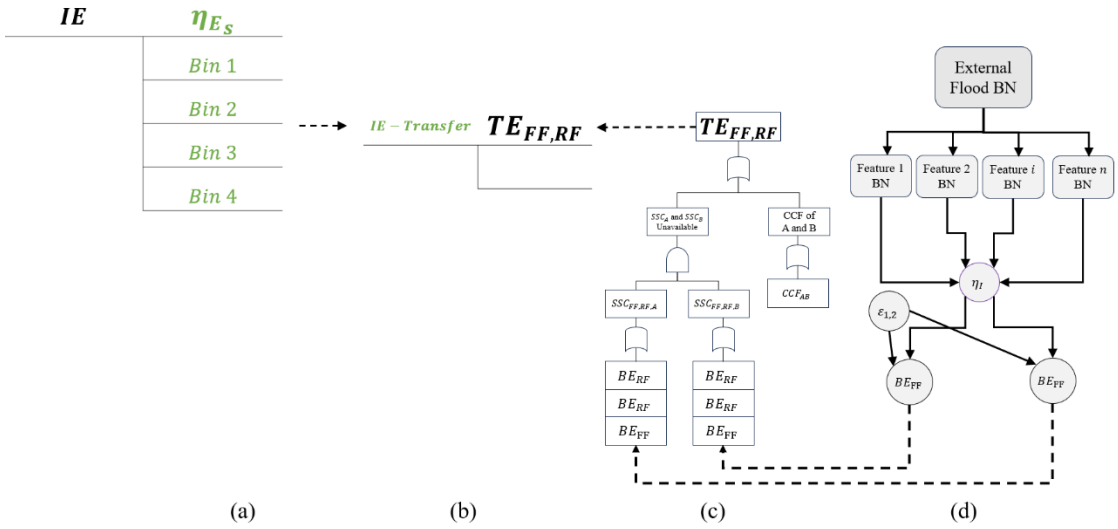

Figure 14: Hybrid Causal Logic Configuration

4.2 Implementation of External Flood Probabilistic Risk Assessment Configurations

4.2.1 Case Study Assumptions

This work implements each configuration described in Section 4.1 for a case study application using GeNIe [85] and SAPHIRE [86]. The case study focuses on a single building with a set of flood protection features, which consists of three penetration seals with varying installation heights, and a door protected by a floodgate at plant grade. The case study configuration assumptions are labeled in Figure 15 and are defined to provide meaningful results, but do not reflect any NPP site. Flood modeling assumptions and probability distributions are defined as in Shen et al. [1]. Flood feature performance and random failure assumptions are sourced from industry-wide average databases by Ma et al. [85], Ma et al. [88], and Zhang et al. [89].

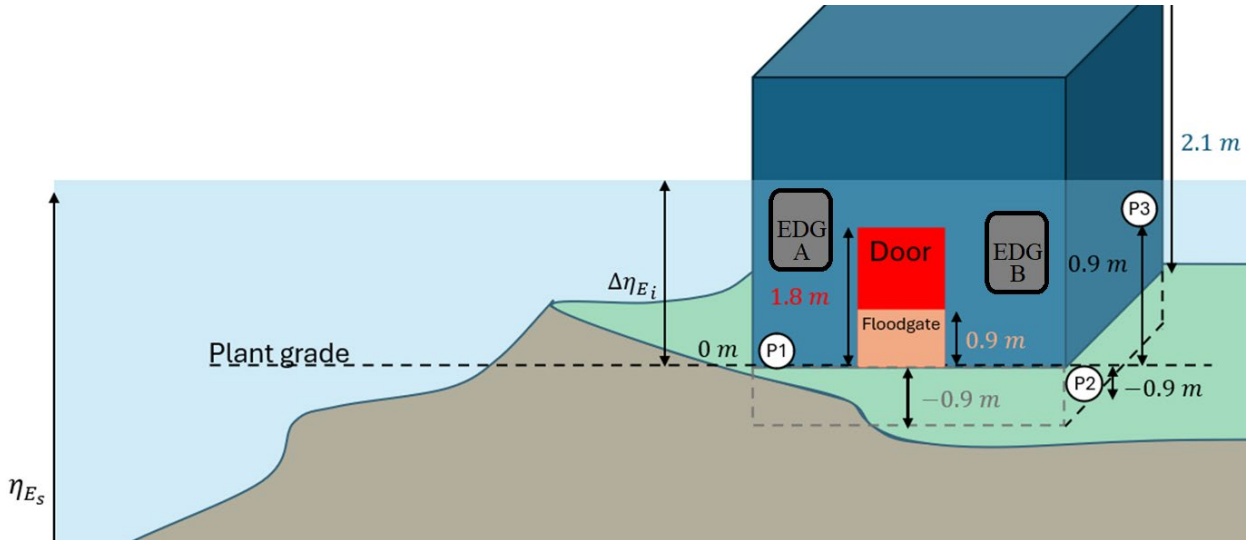

Figure 15: Case Study Site Characteristics

The site has a variable topography that alters the local flood elevation, which is propagated across the site with a bath-tub approach [68]. The flood imposes a demand on the building envelope, including flood protection features. If the flood protection features are degraded or damaged, water enters the interior of the building, which is partially buried with a floor at $0.9\ m$ below grade. The building houses two EDGs, which make up the emergency power system (EPS). The case study assumes the flood causes a loss of offsite power (LOOP). Thus, the PRA focuses on modeling a station blackout (SBO) that is initiated if the EDGs are inundated by the flood.

The failure of the EPS is separately represented as a flood-induced failure (EPS_{FF}) and random failure (EPS_{RF}). Flood fragility of electrical components is typically modeled as a cliff-edge, assuming failed or not failed [21]. In this case study, EDGs are assumed to be raised around

$0.3\ m$ from the interior floor of the room, with critical components housed at this height or greater. The assumed probabilities of EPS failure are defined as a function of flood depth within the room. These assumptions include a moderate failure probability for flood depths below 0.3m to account for the effects of factors such as humidity and splashing. The failure probability increases towards 1 as the elevation increases, assuming some capacity of the EDGs to operate partially submerged. Therefore, given the nature of electrical failures from floods, EPS_{FF} in the FT is a single top event probability, or a single node CPT in the BN. The failure probability distribution of the EDGs is given as $P(EPS_{FF} = Fail|\eta_I) = [0, 0.1, 0.2, 1]$ for internal flood height bins $\eta_I = [0\ m, 0\ to\ 0.3\ m, 0.3\ m\ to\ 1.5\ m, 1.5\ m\ to\ 3\ m]$.

Random failures of the EDGs are modeled as failure to start (FTS), failure to run (FTR), testing and maintenance (TM), and CCFs, with probabilities defined based on industry averages [85] [88] [89]. The logic of the EPS failure can be represented either by an FT (Figure 16a) or a BN (Figure 16b). The two models are logically and quantitatively equivalent. The logic OR gates of the intermediate events "EDG A Unavailable" and "EDG B Unavailable" are represented by the events $EDG_{A,RF}$ and $EDG_{B,RF}$, and the AND gate of A and B Unavailable is represented in EPS_{RF}. Both EDGs cannot be tested or maintained, and therefore the gate is represented as an XOR gate. Additionally, Figure 16b leverages the conditional probability abilities of the BN, and represents CCFs through causal logic as seen in the links between the failure modes of EDG A to EDG B.

More details for quantifying these conditional CCFs are provided in Appendix B: Conditional CCF Discussion and Example.

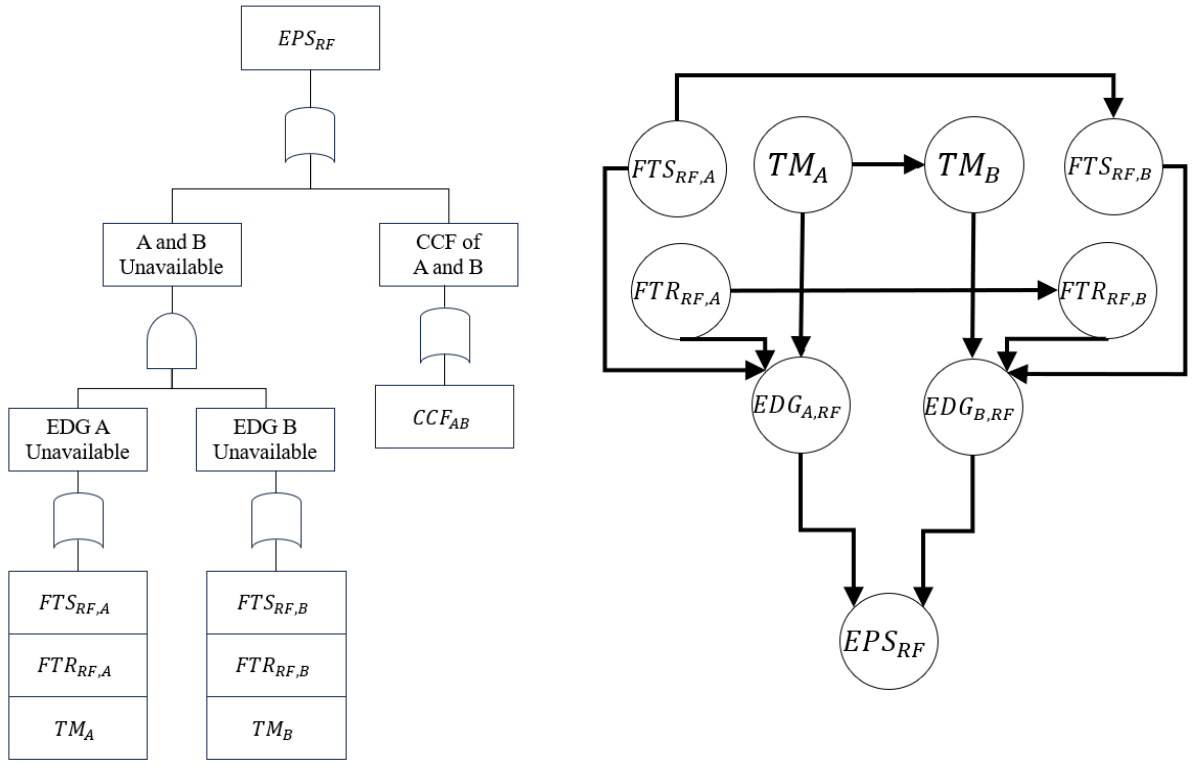

(a) FT Model (b) BN Model

Figure 16: Probabilistic Graphical Models of the EPS_{RF} Failure

The following sections implement each configuration presented in Section 4.1 for the case study modeling flood-induced SBO. This case study focuses on the flood effects, showing how the information from a BN model can be strategically "connected to" ETs and FTs in an external flood context. The following sections describe the process of developing ET/FT models for various

configurations that incorporate the probabilistic information from the BN that cannot be generated directly using only ET/FTs. To convert the BN logic (Configuration 1) to ET/FT logic (Configuration 2) and hybrid logic (configurations 3 and 4), systematic processes described by Bobbio [90] are used along with forward inference to generate marginalized conditional probabilities, and aggregation of multiple states into binary states. The subsections that follow describe the implementation of each configuration and provide commentary on the identified implementation advantages of each.

All resulting configurations have been implemented and quantified in GeNIe [85] and SAPHIRE [86] to verify they are logically and quantitatively equivalent through comparison of computed SBO and intermediate probabilities. The only discrepancy arose in rounding errors of the respective tools.

4.2.2 Configuration 1: Monte Carlo Augmented Bayesian Network

4.2.2.1 Configuration 1 Implementation

The BN formulation of Configuration 1 (as described in Section 4.1.1) serves as the basis of the logic and source of probabilities for developing logically and quantitatively equivalent models for all other configurations. The BN logic (reflected by the BN shown in Figure 17) was constructed to model the flood-induced SBO scenario, and the CPTs were generated using the

assumptions in Shen et al [1]. The SBO is initiated by a flood-induced LOOP, hence the link from η_{E_S} to LOOP. The flood failures of the two EDGs are represented by $EDG_{FF,A}$ and $EDG_{FF,B}$.

The BN was selected as the baseline for all configurations because it offers the greatest flexibility in modeling, capable of showcasing not only its own improvements on flood modeling, but also limitations in ETs and FTs. Specifically, the BN can improve on flood modeling in PRAs and overcome several limitations in ETs and FTs, such as the binary state assumption and statistical dependencies.

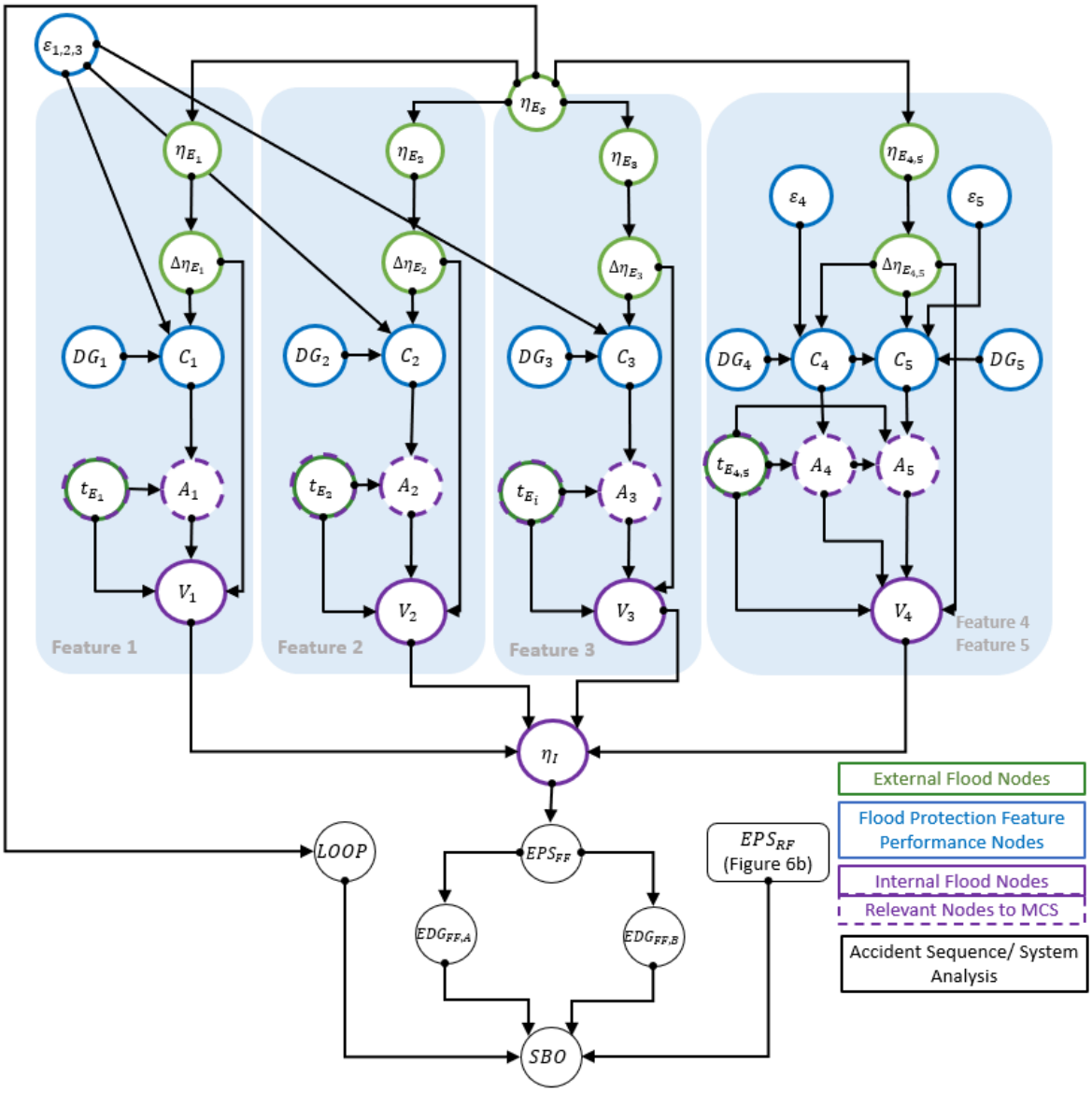

Figure 17: Configuration 1 Implementation

4.2.2.2 Configuration 1 Commentary

The MC-BN approach has advantages that improve flood modeling and address assumptions in ETs and FTs. First, the BN can visually represent causal relationships between variables using nodes and directional links. The familial terminology of parent and child nodes makes it possible to communicate the direction of influence from causes to effects. This allows practitioners to transparently represent diverse types of dependencies and how uncertainty propagates through the model. The BN also enables efficient multi-directional inference (i.e., calculating the probability of a cause given an observed effect, and vice versa), which allows for the exploration of probabilities considering the evidence cases. This supports sensitivity analyses, can be used to calculate importance measures, and can be used to perform other exploratory assessments to support RIDM.

While the BN offers many benefits for external flood PRA modeling, it can easily become complex and computationally demanding (in memory) as more nodes and states are represented in the BN. Generating the nodes of the BN can also be extensive and requires not just the effort in developing a complete scope PRA, but also the effort in modeling distributions to represent causal dependencies. Furthermore, most of the existing PRA experience is in ETs and FTs, and transitioning to a BN-based PRA framework would require a significant effort in translating plant-specific models.

4.2.3 Configuration 2: ET/FT Approach Using MC-BN Derived Probabilities

4.2.3.1 Configuration 2 Implementation

The logic and quantification of Configuration 2, in which the BN is simplified to ETs/FTs. Thus, configurations 1 and 2 are logically and quantitatively equivalent, these configurations provide the same insights because the BN probabilities are coalesced into the branch probabilities. Quantitative differences are due to differing quantification methods between software and rounding. The resulting ETs are represented in Figure 18(a)-(d) and are obtained as described below:

a) The external flood initiator ET (Figure 18a) has branches corresponding to external flood ranges, where the discretization and probabilities are directly copied from the η_{E_S} node. Each initiator bin of η_{E_S} transfers into a unique flood protection performance ET.

b) The flood protection performance ET (Figure 18b) connected to each external flood SSC response ET includes or omits flood protection features based on whether they can be affected by floods within the initiator bin range. The branches corresponding to the binary state of each feature with failure probabilities obtained by setting evidence in the BN. To obtain the probabilities of the flood protection feature failures C_i within each external flood initiator-specific ET, evidence is set for each state of node η_{E_S} to correspond to the relevant flood range and the resulting updated distribution of the flood protection node is extracted. Because the ET requires binary states, the

probability assigned to the failure state for each feature represents the sum over the probabilities associated with all damage states in the BN.

c) The internal flood depth ET (Figure 18c) is conditioned on the unique state combinations of flood protection features, and the branch probabilities of internal flood depth ET are also updated by the resultant probability distribution of η_I, with uncertainties propagated from the evidence cases of η_{E_S}. This provides a strategy for calculating conditional failure probabilities for use in the ET that account for intermediate nodes models in the BN that are not included in the ET (e.g., $\eta_{E_i}, \Delta\eta_{E_i}, DG_i, \varepsilon_{1,2,3}$).

d) The external flood SSC response ET (Figure 18d) is the final ET that models the safety-related SSC performance, representing failures from flood-induced or randomly induced failures, given the internal flood height. The probabilities of this ET are sourced from the assumptions to produce meaningful results.

Each transfer ET is unique, given its previous transferring ET branch. This creates a very large model. In the interest of presentation, Figure 18 only shows the pathway of a single end state of SBO. Other branch pathways are not shown for visual simplification. This pathway assumes an external flood elevation between 1.8 and 2.7 meters, which affects a unique feature configuration consisting of penetration seals 1 (P_1) and 2 (P_2), and the door-protected floodgate (FG). This ET

transfers to a unique internal flood distribution. The pathway continues to follow the most extreme case of an internal flood of 1.5 to 3 meters, which then leads to top events EPS_{FF} and EPS_{RF}.

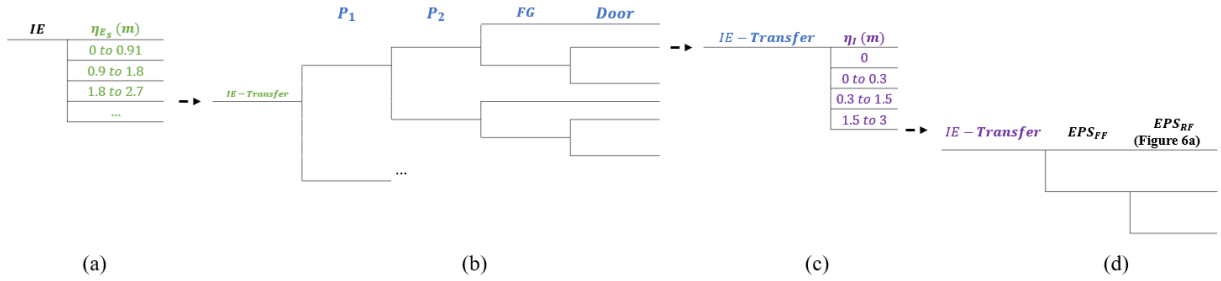

Figure 18: Configuration 2 Implementation

4.2.3.2 Configuration 2 Commentary

ETs and FTs reflect current PRA practice, are well documented, and widely used in the nuclear industry. They have supported RIDM, particularly for internal events. However, they can limit external flood modeling because of the binary state assumption limited capability to model complex dependencies. Moreover, the process of manually developing each unique pathway's logic and inserting branch probabilities can require substantial effort and lead to human error in data entry. In contrast, the BN offers a more compact and visual representation. Furthermore, SAPHIRE approximates failure probabilities to about four significant figures, whereas GeNIe quantifies to about eight significant figures. The higher number of significant figures is beneficial for BNs when for uncertainty propagation across the model, allowing the representation of the accumulation of small but potentially many sources of uncertainty.

4.2.4 Configuration 3: External Flood MC-BN Hybrid Approach

4.2.4.1 Configuration 3 Implementation

The logic and quantification of Configuration 3 leverages both the BN and ET/FT, effectively integrating parts of Configuration 1 and Configuration 2. Specifically, Configuration 3 delegates the external flood modeling within the BN, while the other portions of the models are modeled using the ET/FT framework. The cutsets obtained in Configuration 3 are the same as Configuration 4, except for cutsets from the flood protection feature ET, whose quantification and representation are delegated to the BN.

The Configuration 3 ET/FT framework begins with the external flood SSC response ET (Figure 19a), obtained as described in Section 4.1.3. However, in Configuration 3, the external flood SSC response ET transfers directly to the internal flood depth ET (Figure 19b), and the flood protection performance ET described in Section 4.1.2 is replaced by portions of the BN that model flood propagation and flood protection feature performance, as shown by the BN at the top of Figure 19. The branch probabilities for the internal flood depth ET corresponding to each initiating bin are obtained by setting evidence on the node η_{E_S}, propagating that evidence throughout the BN to obtain resultant η_I probability distribution, and entering the resultant state probabilities on the branches of the internal flood depth ET. Similar to Configuration 2, each bin of the internal flood depth ET subsequently transfers to an external flood plant response ET (Figure 19c).

As is the case with Configuration 2, each state generates many branches in each ET. Therefore, to simplify the presentation, only a select number of branches and transfers are provided in Figure 19. The selected pathway assumes an initiator bin of $0.9\ m$ to 1.8 m, resulting in an internal flood depth of $1.5\ m$ to $3m$, which can then induce a binary flood failure of EPS_{FF} alongside the possibility of it randomly failing, which is represented in EPS_{RF}.

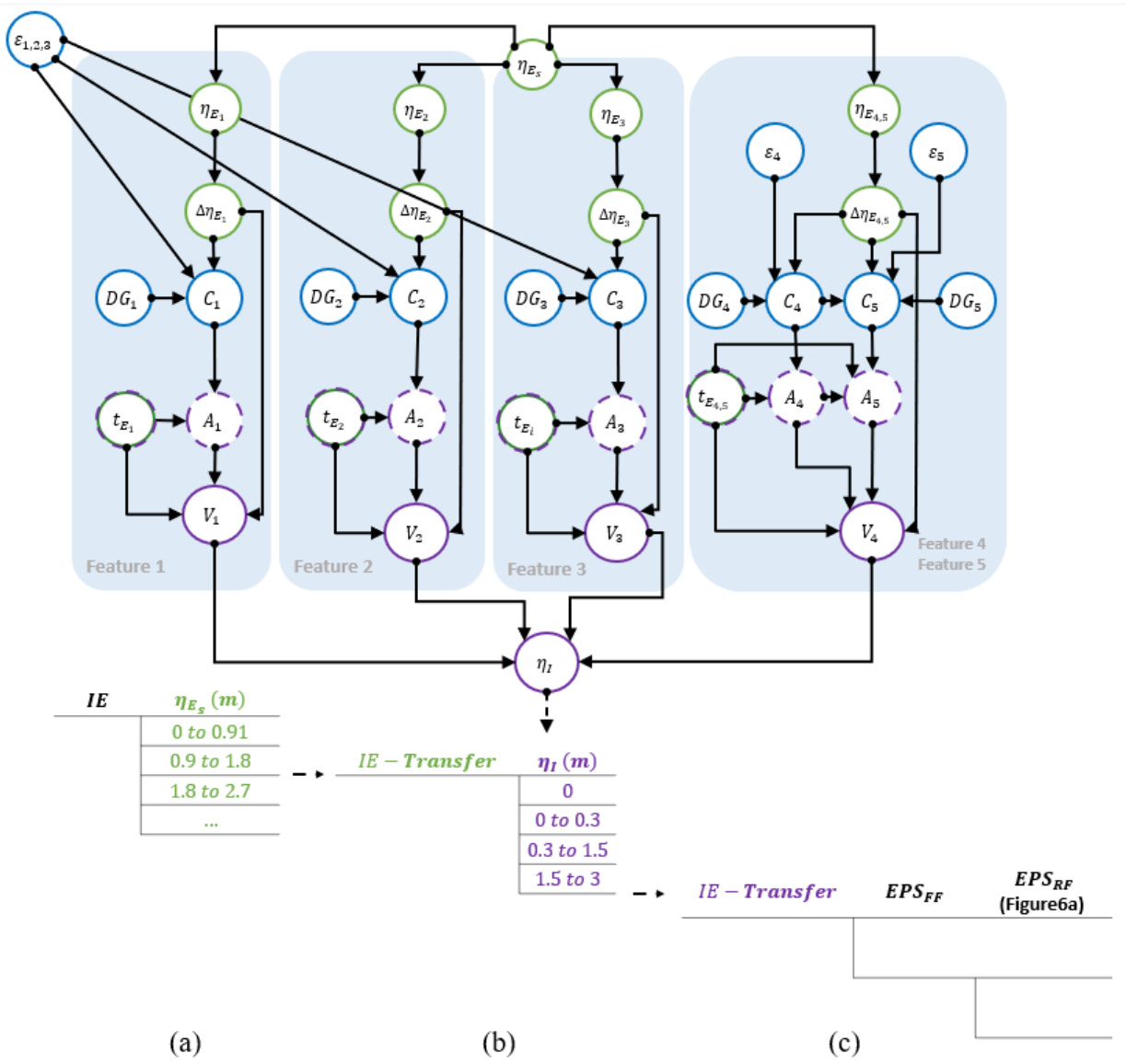

Figure 19: Configuration 3 Implementation

4.2.4.2 Configuration 3 Commentary

This hybrid configuration takes advantage of the BN's ability to refine the flood model and address its complexities by modeling multiple states, incorporating temporal and spatial dependencies, and explicitly including a diverse set of variables such as fragility error or degradation. However, this hybrid model limits the capability of Bayesian updating, which allows for the prediction and diagnosis of resulting states given evidence queries at the integration point between the BN and ETs/FTs. Delegating the external flood to the external flood allows the practitioner to more comprehensively develop the external flood model. This provides more insights into the evolution of the external flood, leaving the flood's effects on the site to the more simplified ET/FT model. This can provide a more comprehensive risk model and enable more efficient exploration of flood scenarios to support RIDM.

This configuration significantly reduces the effort in manually defining the unique branch pathways of the flood protection feature ETs. This multi-branch ET can still require a large model, which is made exponentially larger as the ETs are separately modeled for each initiator bin. This creates challenges in quantification efficiency, difficulty in traceability and navigation, and requires more resources to develop. This limitation may be impractical for a finer binning of external and internal flood heights.

4.2.5 Configuration 4: Hybrid Causal Logic Approach

4.2.5.1 Configuration 4 Implementation

Like Configuration 3, the logic and quantification of Configuration 4 leverages the BN and ET/FT, generating and quantifying the same cutsets as the previous configurations, as the flood protection feature ETs and internal flood ETs are coalesced into the safety-related flood fragility nodes. However, they differ in the integration point of the BN. Specifically, the BN is used to model flood protection feature performance (as in Configuration 3) as well as the flood performance of safety-related SSCs. Safety-related SSCs performance aspects not related to the flood event are modeled in an initiator-bin specific ET. Thus, the BN integration point is set at the basic events representing the flood performance of the EDGs in the FT (Figure *20*c), $\mathrm{EDG_{FF,A}}$ and $\mathrm{EDG_{FF,B}}$. These basic event probabilities are obtained by setting evidence at the node η_{E_S} corresponding to each bin of the external flood initiator ET as previously done in the other configurations and extracting the resulting updated failure probabilities of the nodes $\mathrm{EDG_{FF,A}}$ and $\mathrm{EDG_{FF,B}}$. Thus, the FT shown in Figure *20*c models both the random performance of the EPS (i.e., FTS, FTR, TM) and integrates the logic of random and flood-induced failures in the EPS FT (i.e., $\mathrm{EDG_{FF}}$), in top event $\mathrm{EPS_{RF,FF}}$ as input to the external flood plant response ET (Figure *20*b). As in Configuration 3, this ET is transferred from the external flood initiator ET (Figure *20*a). Figure *20* presents this logic, following the path of an initiator bin from $0.9m$ to $1.8m$.

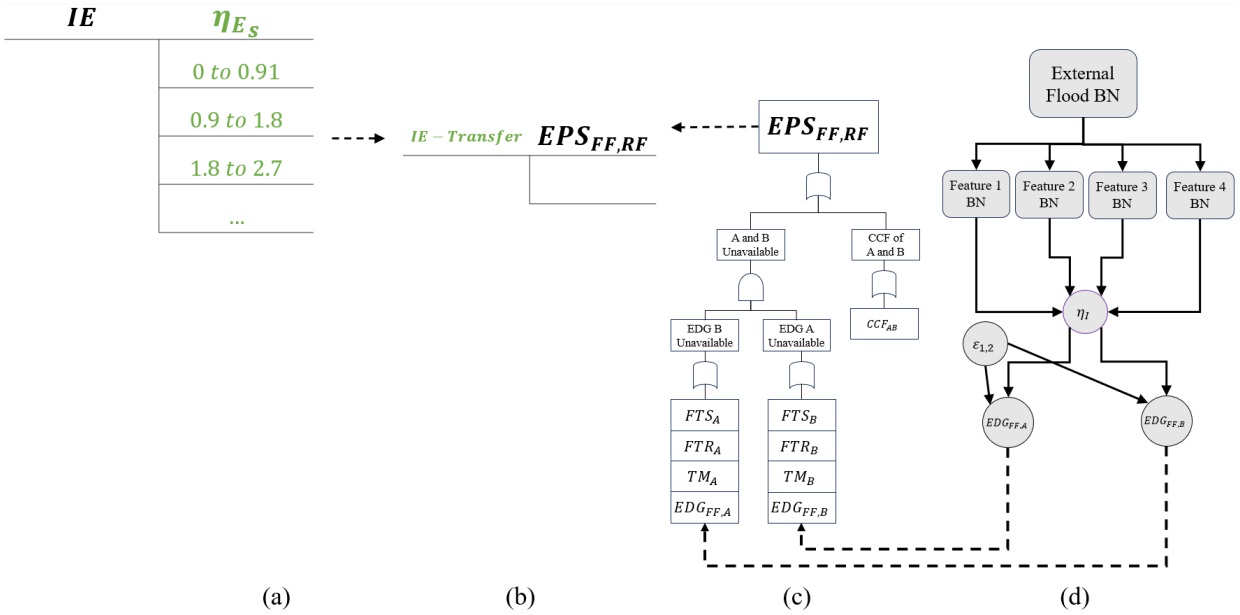

Figure 20: Configuration 4 Implementation

4.2.5.2 Configuration 4 Commentary

This configuration delegates most of the flood-related modeling to the BN and integrates the results into a basic event within the $EPS_{FF,RF}$ FT. While this reduces the results of the BN to a binary state, it retains the causal relationships of all previous nodes conditioned on the external flood. This approach is appropriate when there is a need to focus on the effects of flood-induced failures, such as sensitivity analyses or understanding the impact of flood events. This approach allows the practitioner to isolate the performance of flood protection features given the demand of floods.

The manual branch probability insertion is more straightforward than Configurations 2 and 3, reducing errors in transferring probabilities. As most of the states are represented in the BN, this makes the configuration easier to navigate by leveraging the visual transparency of the BN, further reducing the size of the ETs.

4.3 Summary and Conclusion

This work provides four logically and quantitatively equivalent configurations of hybrid external flood PRAs, with varying levels of integration of conventional and BN methods. Configurations 1 and 2 illustrate the capabilities, benefits, and limitations of BNs and ETs/FTs regarding external flood modeling. Hybrid configurations 3 and 4 provide different strategies to integrate the BN into the ET/FT models, thus enabling the benefits of both modeling methods.

Each configuration is implemented using a case study and assessed for advantages and challenges. The full BN model of configuration 1 is appropriate when practitioners are interested in capturing the complexity of external flood modeling (e.g., complex dependencies and failure states), expanding on random failure modeling assumptions, and enabling multi-directional inference. It is best to see a high-level overview of the uncertainty propagations while preserving the level of detail. However, this model is feasible only if the resources are available to build and run BN-based plant models. Conversely, the ET/FT of configuration 2 preserves logic structures used for existing PRAs for NPPs. However, it requires an extensive set of limiting assumptions and results in the need to develop large ETs. Configuration 3 modeling the external flood in the

BN which provides a more focused view on the external flood effects and resultant failure. It then simplifies this result to become an input to the ET/FT structure, which will lose the level of detail on its impact on the end consequences. Configuration 4 of the hybrid causal logic makes selective use of BNs for specific PRA modeling aspects. It delegates all flood considerations, including the external flood and external flood failures in the BN, increasing the level of detail on the flood's impact. However, this still simplifies the end probability into a binary state, obfuscating multiple flood-induced damage states. The proposed configurations either lean towards delegating the model more to the BN or the ET/FTs. This paper outlines practical strategies for enabling this integration and offers commentary on implementation challenges. This facilitates a gradual transition to improving the conventional model while preserving decades' worth of knowledge and experience. A summary of these insights is provided in Table 7.

Table 7: Summary of Configuration Insights

Configuration		Configuration Insights
Number	Name	
1	MC-BN Approach	• Full Bayesian updating capabilities for sensitivity and importance analyses • Traceable for quantifying and visualizing uncertainty propagation across the BN • Supports RIDM through exploration of external flooding conditions, plant effects and non-flood related aspects through Bayesian updating • High computational and memory demands • Intensive modeling effort, easy to verify through quantification of intermediate probabilities and risk contributors • Not widely implemented in the nuclear industry
2	ET/FT Approach Using MC-BN Derived Probabilities	• Well documented and widely used in the nuclear industry • Supports RIDM through exploration of functional relationships between initiator bins and plant effects through sensitivity analyses and importance measures • Limiting assumptions in flood modeling • Intensive modeling effort, difficult to verify through quantification of intermediate probabilities and risk contributors
3	External Flood MC-BN Hybrid Approach	• Full capabilities of the BN to the external flood for sensitivity and importance analyses • Supports RIDM by enabling exploration of external flooding conditions through Bayesian updating • Less intensive modeling effort to generate, easier to verify BN and ET/FT through quantification of intermediate probabilities and risk contributors
4	Hybrid Causal Logic Approach	• Applies BN capabilities to the external flood and flood fragility of safety-related SSCs for sensitivity analyses and importance analyses • Supports RIDM through exploration of external flooding conditions and plant effects through Bayesian updating • Less intensive modeling effort to generate, easy to verify BN and ET/FT through quantification of intermediate probabilities and risk contributors

Chapter 5. Conclusion

External flood events can damage flood protection features, allowing water to infiltrate plant structures and damage safety-related SSCs. Flood-related operating experience has highlighted the potential challenges that plants may have to mitigate the impact of floods across the NPP site. While there is a recognized need to probabilistically assess the risks from external flood events, few external flood PRAs have been performed in the U.S. Flood risks have yet to be commonly assessed due to their complex nature, originating from a range of causes, and highly site-specific nature. This motivated the fulfillment of a research need in developing a more comprehensive probabilistic approach to analyzing external flood risks.

To better understand the challenges practitioners face when assessing risks from external floods and other hazards, a questionnaire was distributed to the PRA community to collect insights regarding needs and trends related to PRA modeling within the nuclear industry, in which the questions are provided in Appendix A: Questionnaire Questions. The results of the questionnaire provided insights into the need to improve SSC dependency modeling, incorporating Bayesian updating, and expanding the scope to external events. These insights led to the development of an MC-BN and hybrid modeling framework that addresses challenges identified by the PRA community while preserving knowledge and experience of conventional PRA modeling tools (i.e., ETs and FTs).

Specifically, this dissertation develops an external flood PRA framework that meets the three primary objectives:

Objective 1: Develop a PRA modeling approach that complements the deterministic approach of analyzing external flood risks by enabling inclusion of physical relationships regarding the effects of the flood hazard across the site.

This dissertation developed an external flood PRA framework that incorporates physical relationships to develop the logic structure of the MC-BN and the conditional relationships. Section 3.3 illustrates how the MC-BN's logic is shaped by deterministic physical characteristics of the site. For example, the external flood elevation considers the topography of the site and flood protection feature elevations and calculates external flood depth based on site features. These physical relationships allow the observation of the propagation of uncertainty over the site. Deterministic methods were also used to quantify the impact of degradation state DG_i on flood protection feature state C_i through the pre-existing degradation factor $P_{i,k}$. Physical relationships established the integration of relevant nodes in Section 3.3.7, enabling the augmentation of the BN to reduce computational and memory demands and discretization errors. Deterministic strategies that have been applied in other applications have also been used to generate CPTs to develop probabilistic assumptions such as the HCLPF approach.

Objective 2: Develop a PRA modeling approach that captures relevant external flood modeling considerations that cannot be directly included within the conventional modeling approach (e.g., temporal and spatial, in addition to conventional CCF dependencies, and multiple damage states).

Through the inherent characteristics of the MC-BN, the proposed modeling approaches address several challenges, such as dependencies and binary damage state assumptions, which affect practitioners' ability to use conventional tools for external flood PRA. In the proposed framework, temporal dependencies are represented in the causal relationships of flood duration. The spatial dependencies are represented in the multiple causal relationships from external flood elevation to internal flood depth. The MC-BN effectively represents causal relationships by propagating evidence throughout the model, enhancing sensitivity analyses, and better accounts for spatial and temporal variability. The MC-BN also enables the use of multi-state nodes, which increases the resolution with which SSC degradation and damage can be modeled.

Objective 3: Develop a PRA modeling approach that includes strategies to interface the novel framework with conventional ETs and FTs and compare the advantages and challenges in the strategy.

A hybrid external flood PRA framework was developed to leverage the benefits of both ETs and FTs, and MC-BNs. Several strategies to enable the integration of an MC-BN with ET/FTs are proposed through a series of logically and quantitatively equivalent hybrid models. A case study application is used to demonstrate the proposed strategies, implement them using commonly

used software applications, verify consistency in numerical results, and develop lessons learned/commentary regarding their advantages and disadvantages.

5.1 Summary of Contributions

This dissertation develops novel external flood PRA methods that address several identified challenges associated with conventional tools, supporting risk-informed decision-making regarding plant operations and safety.

The external flood MC-BN incorporated insights from the literature and questionnaire results, capturing the gaps in research and trending needs in the PRA community. The MC-BN improves upon several assumptions in conventional risk tools that affect external flood modeling. Specifically, the MC-BN enables modeling some aspects that capture the temporal evolution of floods and spatial heterogeneity, which provides a more realistic representation of the impact of the flood demand on flood protection features across the site. The ability to capture multiple states for each node offers greater detail on SSC performance, enhancing the resolution with which flood effects and SSC performance can be modeled. Challenges related to dependency modeling are addressed through causal relationships in the conditional probability distributions of the BN, representing the impact of floods more realistically. The BN's inherent capability for Bayesian updating allows practitioners to communicate risk for evidence cases and supports risk-informed decisions.

The hybrid external flood framework provides a means to leverage advantages in the MC-BN while preserving strategies and tools in the conventional external flood PRA model. The extent to which the MC-BN is leveraged in the external flood PRA can garner different insights, given the integration point of the novel and conventional risk tools. As more of the PRA model is delegated in the MC-BN, the uncertainty propagation and Bayesian updating capabilities can be used to make risk-informed decisions. However, the trade-off is the effort and resources required to generate a comprehensive MC-BN. Therefore, the configurations can optimize that trade-off given the needs of the NPP site.

- Configuration 1 is appropriate when resources are available to develop a full-scope external flood PRA with the MC-BN approach. It provides a detailed and traceable model to quantify the propagation of uncertainty and leverage Bayesian updating for sensitivity and importance analyses.
- Configuration 2 is appropriate when the limitations of the conventional framework will not adversely affect the ability of the model to support the RIDM application. It is particularly beneficial when an existing PRA (using ETs and/or FTs) is available on which to base the external flood PRA [18].
- Configuration 3 is appropriate when enhanced modeling the external flood and state of the flood protection features are needed. This configuration provides a focused view of the external flood event evolution and is suitable for providing a more

detailed distribution of the internal flood depth distribution, while retaining other modeling aspects within the conventional models.

- Configuration 4 is appropriate when there is a need for enhanced modeling of the external flood event and flood-induced failures of flood protection features as well as safety-related SSCs. This expands the diagnosis and prognosis abilities to provide more details in the sensitivity and importance analyses, focusing on flood fragility on relevant SSCs.

5.2 Future Research

Several opportunities for enhancement and future work have been identified. The work presented in this dissertation considers a single flood hazard. However, flood hazards (e.g., seismic-induced dam failure or LIP and storm surge induced by a single hurricane) can occur in a coincidental, correlated, or consequential manner, leading to differing effects on the NPP site than single hazards. Modification of the proposed framework to address combined hazards would require a more in-depth look into the flood mechanisms and their combined effects, requiring a coupled assessment to represent the flood characteristics. Several existing studies (e.g., Mohammadi [2] and Liu [91]) provide resources that can inform further development of models that can address combined hazards within the proposed hybrid framework.

Furthermore, this work incorporated system dynamics through temporal dependencies, which linked the flood duration to the external flood elevation and subsequent child nodes; however, it does not explicitly model the system's dynamics through time-dependent variables. This would allow the assessment to be more realistic. For example, warning time is a critical variable in plant response, particularly when a plant's flood response strategy involves substantial human actions (e.g., placing temporary flood protection features). The inclusion of human reliability would result in a more comprehensive model capable of assessing a broader set of uncertainties but would require expansion of the model to include HRA considerations.

Further work can be done to optimize the quantification efficiency of the MC-BN, reducing the computational and memory demands for large and complex BNs that use a converging BN structure in which a single child node has many parents. This converging structure can potentially be rearranged to a chain structure, as was done by [92]. However, further work is needed to enable use of chain structures with a multi-state rather than binary state nodes.

Appendix A: Questionnaire Questions

The questionnaire was sent to 431 members of the international PRA community in early 2022 and recorded 52 responses. The questionnaire was sent to practitioners within industry, academia, international labs, government agencies, and independent contractors, although the demographics of respondents are unknown due to anonymity. Based on the responses to question 5, respondents are engaged in a diverse scope of PRAs such as internal and external hazards, levels 1-3, or dynamic PRAs at various power levels. Additionally, the questionnaire gathered practitioner insights on the advantages and limitations of PRA software and other tools.

The questionnaire contained seven questions. Question 1 was multiple selection, while the remaining questions were open-ended:

1) What static PRA software do you have experience using? Select multiple if applicable.
    a. SAPHIRE
    b. Riskman
    c. RiskSpectrum
    d. CAFTA
    e. WinNUPRA
    f. FRANX
    g. Other (Please Specify)
    h. I do not use PRA tools

2) What are the strengths of the PRA software/tools you are using/have used? If you discuss multiple tools, please connect each tool to its strengths.
3) What are the limitations of the PRA software/tools you are using/have used? If you discuss multiple tools, please connect each tool to its limitations.
4) What other tools or software have you used to supplement the PRA tools/software you identified above? Why have they been needed? If you discuss multiple tools, please connect each tool to its necessity.
5) What types of PRAs have you worked on when using the tools/software/methods identified above? (e.g., internal events, internal flooding, fire, seismic, high winds, external flooding, human risk assessment (HRA), data analysis, level II/III,...)
6) What types of nuclear power technologies do you work with when using the tools/software/methods identified above? (e.g., LWRs, SMRs, gas reactors, breeder reactors, molten salt reactors,...)
7) Please provide additional comments regarding the potential for new or existing PRA tools (used within or outside the nuclear industry) to meet the evolving needs of the nuclear industry.

Appendix B: Conditional CCF Discussion and Example

The conditional CCF can be calculated and represented in the CPT provided the following equations and definitions. Assuming non-staggered testing and applying an alpha-factor model, the probability of a common cause basic event $Q_k^{(m)}$, for component k out of a total of m identical components can be calculated with Equation 6 [24].

$$Q_k^{(m)} = \frac{k}{\binom{k-1}{m-1}} \frac{\alpha_k}{\alpha_t} Q_t \qquad \text{Equation 6}$$

Q_t is the total failure probability for m components due to all independent and common cause events, α_t (Equation 7) is provided below, and should equal unity as it is the total fraction of failures that occur among m components, while α_k (Equation 8) is the fraction of the frequency of k out of m failures occur.

$$\alpha_t = \sum_{k=1}^{m} k\alpha_k = 1 \qquad \text{Equation 7}$$

$$\alpha_k = \frac{n_k}{\sum_{j=1}^{m} n_j} \qquad \text{Equation 8}$$

Where n_k is the number of failures for component k, which is over the sum of all failures n_j where $1 < j \leq m$. α_k is also the conditional probability of k components given a failure has occurred in a group of m identical components, which can be expressed in Equation 9.

$$\alpha_k = \Pr\left(P_m | P_k\right) \quad \text{Equation 9}$$

Where P_k is the event of common cause failure of k components out of m, and P_m is the event of failure of component m out of m irrespective of any dependency in their failure.

Example of Conditional Common Cause Failure Probability of EDG_A and EDG_B Leveraging the Alpha Factor Model

The conditional CCF calculation is demonstrated on the CCF, assuming an alpha factor model for the failure mode of the EDGs failing to start (FTS). This calculation is applied to the two EDGs in the BN and therefore assumes m = 2, as there are two EDGs A and B in the system. Therefore, the failure of the system Q_s can be calculated as follows:

$$Q_s = \Pr(A) \cdot \Pr(B) + \Pr(CCF_{AB}) = (Q_1)^2 + Q_2 \quad \text{Equation 10}$$

Where events A and B are the failure of EDG A and B, respectively, and CCF_{AB} is the common cause failure of EDG A and B. Leveraging Equation 10, Q_1 and Q_2 can be calculated with the following:

$$Q_1 = \frac{\alpha_1}{\alpha_1 + 2\alpha_2} Q_t \quad \text{Equation 11}$$

$$Q_2 = \frac{\alpha_2}{\alpha_1 + 2\alpha_2} Q_t \quad \text{Equation 12}$$

Therefore, given Equation 11 and Equation 12, Q_s for EDG A and B is calculated in Equation 13.

$$Q_s = \left(\frac{\alpha_1}{\alpha_1+2\alpha_2} Q_t\right)^2 + \frac{\alpha_2}{\alpha_1+2\alpha_2} Q_t \quad \text{Equation 13}$$

Note that Q_s in this context can also be defined as Equation 14.

$$Q_s = \Pr(A \cap B) = \Pr(A) \cdot \Pr(B|A) = Q_1 \cdot \Pr(B|A) \quad \text{Equation 14}$$

While $Q_2 < Q_1$ and $Q_1 \approx Q_t$, the system failure can be approximated as $Q_s \approx Q_t \cdot Pr(B|A)$. This allows us to approximate the quantity to Equation 14 as seen in Equation 15.

$$Q_t \cdot \Pr(B|A) \approx \left(\frac{\alpha_1}{\alpha_1 + 2\alpha_2} Q_t\right)^2 + \frac{\alpha_2}{\alpha_1 + 2\alpha_2} Q_t \quad \text{Equation 15}$$

Isolating Pr $(B|A)$, we obtain Equation 16.

$$\Pr(B|A) \approx \left(\frac{\alpha_1}{\alpha_1 + 2\alpha_2}\right)^2 \cdot Q_t + \frac{\alpha_2}{\alpha_1 + 2\alpha_2} \quad \text{Equation 16}$$

Assuming the EDGs are failed due to the failure mode of failure to start (FTS), the rate of failure for an EDG $Q_t = 2.22E-3$, and the alpha factors of $\alpha_1 = 0.9917164$ and $\alpha_2 = 8.28E-3$, which are taken from industry averages [87] [89]. The general CPT for EDG B FTS is provided in Table 8.

Table 8: General CPT of Failure to Start for EDG B

	$\bar{A}$	A
$\bar{B}$	Pr $(\bar{B}\|\bar{A})$	Pr $(\bar{B}\|A)$
B	Pr $(B\|\bar{A})$	Pr $(B\|A)$

Applying Equation 16, we can obtain $\Pr(B|A)$ and $\Pr(\bar{B}|A)$ as the following:

$$\Pr(B|A) \approx \left(\frac{\alpha_1}{\alpha_1 + 2\alpha_2}\right)^2 Q_t + \frac{\alpha_2}{\alpha_1 + 2\alpha_2}$$

$$\Pr(\bar{B}|A) = 1 - \Pr(B|A)$$

Because the alpha factor model is based on failures, the relationship for $\Pr(B|A)$ cannot be used for non-failure probabilities. Therefore, to obtain the conditional failure probability for the other cells, the law of total probability is leveraged.

$$\Pr(\bar{B}) = \Pr(\bar{B}|\bar{A}) * \Pr(\bar{A}) + \Pr(\bar{B}|A) * \Pr(A)$$

$$\Pr(\bar{B}|\bar{A}) = \frac{\Pr(\bar{B}) - \Pr(\bar{B}|A) * \Pr(A)}{\Pr(\bar{A})}$$

$$\Pr(B|\bar{A}) = 1 - \Pr(\bar{B}|\bar{A})$$

Therefore, leveraging these equations, the CPT is generated in Table 9.

Table 9: CPT of Failure to Start for EDG B

	$\bar{A}$	A
$\bar{B}$	0.999	0.987
B	0.001	0.013

References

[1] Shen J., Bensi M., and Modarres M., "A Monte Carlo augmented Bayesian network approach for external flood PRAs," *Nuclear Engineering and Design*, vol. 433, p. 113840, 2025, doi: 10.1016/j.nucengdes.2025.113840.

[2] Mohammadi S., Bensi M., Kao SC, and DeNeale S.T., "Multi-Mechanism Flood Hazard Assessment: Critical Review of Current Practice and Approaches and Example Use Case Studies," Nuclear Regulatory Commission, Technical Report NUREG/CR-7296, 2022.

[3] Röwekamp M., Gänssmantel G., and Strack C., "Operating Experience with Hydrological External Hazards and Their Potential Safety Significance," *Journal of Polish Safety and Reliability Association, Summer Safety and Reliability Seminars*, vol. 8, no. 1, 2017, Accessed: Mar. 15, 2021. [Online]. Available: https://yadda.icm.edu.pl/baztech/element/bwmeta1.element.baztech-83d83540-136e-40ae-9d52-b8f779142c92

[4] Jensen J., "St. Lucie Unit 1 re Internal RAB Flooding During Heavy Rain Due to Degraded Conduits Lacking Internal Flood Barriers," NRC, St Lucie Unit 1, Licensee Event Report 14-001-03 (ML14343A405), 2014.

[5] Jamil D.M., "Safe Shutdown Potentially Challenged by an External Flooding Event and Inadequate Design and Configuration Control," Nuclear Regulatory Commission, Licensee Event Report 2006-002–00 (ML062710394), 2006.

[6] *Lessons Learned from the Fukushima Nuclear Accident for Improving Safety of U.S. Nuclear Plants*. Washington, D.C.: National Academies Press, 2014. doi: 10.17226/18294.

[7] Gorbatchev A., Mattei J. M., Rebour V., and Vial E., "Report on flooding of Le Blayais power plant on 27 December 1999," presented at the EUROSAFE 2000: International forum for nuclear safety, Koeln, Germany, 2000. Accessed: Feb. 19, 2022. [Online]. Available: https://www.osti.gov/etdeweb/biblio/20209981

[8] Shen J., Bensi M., and Modarres M., "Review of Operating Experience and Fragility Development During Flooding Incidents at Nuclear Power Stations," in *16th International Probabilistic Safety Assessment and Analysis*, Virtual: American Nuclear Society, Nov. 2021.

[9] Weerakkody S.D., “External Flooding Event Modeling and Risk Quantification.,” Nuclear Regulatory Commission, (ML16264A287), 2016. [Online]. Available: https://www.nrc.gov/docs/ML1626/ML16264A287.pdf

[10] Ferrante F., “External Flooding in Regulatory Risk-Informed Decision-Making For Operating Nuclear Reactors in the United States,” in *Proceedings of PSA 2015, the International Topical Meeting on Probabilistic Safety Assessment and Analysis*, Sun Valley, Idaho: American Nuclear Society, 2015.

[11] “10 CFR Appendix A Part 50,” Nuclear Regulatory Commission, 1954. Accessed: Aug. 03, 2022. [Online]. Available: https://www.ecfr.gov/current/title-10/part-50

[12] “Standard Format and Content of Safety Analysis Reports for Nuclear Power Plants,” Nuclear Regulatory Commission, Regulatory Guide 1.070, Rev. 3, 1978.

[13] “Becoming a Modern, Risk-Informed Regulator,” Becoming a Modern, Risk-Informed Regulator. Accessed: Sep. 18, 2025. [Online]. Available: https://www.nrc.gov/about-nrc/plans-performance/modern-risk-informed-reg

[14] Nuclear Regulatory Commission, “Use of Probabilistic Risk Assessment Methods in Nuclear Regulatory Activities; Final Policy Statement,” *Federal Register*, vol. 60, no. 158, 1995, Accessed: Nov. 01, 2022. [Online]. Available: https://www.federalregister.gov/documents/1995/08/16/95-20237/use-of-probabilistic-risk-assessment-methods-in-nuclear-regulatory-activities-final-policy-statement

[15] Siu N., Stutzke M., Dennis S., and Harrison D., “Probabilistic Risk Assessment and Regulatory Decisionmaking: Some Frequently Asked Questions,” Nuclear Regulatory Commission, Report NUREG 2201 (ML16245A032), 2016.

[16] Kaplan S. and Garrick J.B., “On The Quantitative Definition of Risk,” *Risk Analysis*, vol. 1, no. 1, pp. 11–27, 1981, doi: 10.1111/j.1539-6924.1981.tb01350.x.

[17] Rasmussen N., “Reactor Safety Study An Assessment of Accident Risks in U.S. Commercial Nuclear Power Plants,” Nuclear Regulatory Commission, Technical Report WASH-1400 (NUREG-75/014), 1975.

[18] “Standard for Level 1/Large Early Release Frequency Probabilistic Risk Assessment for Nuclear Power Plant Applications,” American Society of Mechanical Engineering (ASME) and American Nuclear Society (ANS), ASME/ANS RA-S-1.1–2024, 2024.

[19] Porter K., “A Beginner’s Guide to Fragility, Vulnerability, and Risk,” in *Encyclopedia of Earthquake Engineering*, Beer M, Kougioumtzoglou I.A., Patelli E., and Au ISK., Eds., Berlin, Heidelberg: Springer Berlin Heidelberg, 2021, pp. 1–29. doi: 10.1007/978-3-642-36197-5_256-1.

[20] Basu P.C., Ravindra M.K., and Mihara Y., “Component fragility for use in PSA of nuclear power plant,” *Nuclear Engineering and Design*, vol. 323, pp. 209–227, 2017, doi: 10.1016/j.nucengdes.2016.10.018.

[21] Bensi M., Ferrante F., and Philip J., “Assessment of Flood Fragility for Nuclear Power Plants: Challenges and Next Steps,” presented at the 23rd International Conference on Structural Mechanics in Reactor Technology, Manchester, UK, Aug. 2015. Accessed: May 11, 2021. [Online]. Available: https://www.nrc.gov/docs/ML1523/ML15230A490.pdf

[22] Schultz M.T., Gouldby B.P., Simm J.D., and Wibowo J.L., “Beyond the Factor of Safety: Developing Fragility Curves to Characterize System Reliability:,” Defense Technical Information Center, Fort Belvoir, VA, ERDC SR-10-1, 2010. doi: 10.21236/ADA525580.

[23] Goldberg F.F., Haasl D.F., Roberts N.H., and Vesely W., “Fault Tree Handbook,” Nuclear Regulatory Commission, Handbook NUREG 0492 (ML100780465), 1981.

[24] Mosleh A., Rasmuson D.M., and Marshall F.M., “Guidelines on Modeling Common-Cause Failures in PRA,” Nuclear Regulatory Commission, Technical Report NUREG/CR-5485, INELIEXT-97-O 1327, 1998.

[25] Shen J., Bensi M., and Modarres M., “Synthesis of Questionnaire Insights Regarding Current PRA and Additional Tools,” presented at the Probabilistic Safety Assessment and Management Conference (PSAM16), Honolulu, Hawaii, Jun. 2022.

[26] Shen J., Marandi S., Bensi M., and Modarres M., “Synthesis of Insights Regarding Current PRA Technologies for Risk-Informed Decision Making,” in *Proceedings of the 18th International Probabilistic Safety Assessment and Analysis*, Knoxville, TN: American Nuclear Society, Jul. 2023.

[27] Ma Z., Smith C., and Prescott S., “A Simulation-Based Dynamic Analysis Approach for Modeling Plant Response to Flooding Events,” Idaho National Lab, RIL 2022-03, 2022.

[28] Metin A.D. *et al.*, "The role of spatial dependence for large-scale flood risk estimation," *Natural Hazards and Earth System Sciences*, vol. 20, no. 4, pp. 967–979, Apr. 2020, doi: 10.5194/nhess-20-967-2020.

[29] Neal J., Keef C., Bates P., Beven K., and Leedal D., "Probabilistic Flood Risk Mapping including Spatial Dependence," *Hydrological Processes*, vol. 27, no. 9, pp. 1349–1363, 2013, doi: 10.1002/hyp.9572.

[30] Quinn N. *et al.*, "The Spatial Dependence of Flood Hazard and Risk in the United States," *Water Resources Research*, vol. 55, no. 3, pp. 1890–1911, 2019, doi: 10.1029/2018WR024205.

[31] Winter B., Schneeberger K., Förster K., and Vorogushyn S., "Event generation for probabilistic flood risk modelling: multi-site peak flow dependence model vs. weather-generator-based approach," *Natural Hazards and Earth System Sciences*, vol. 20, no. 6, pp. 1689–1703, 2020, doi: 10.5194/nhess-20-1689-2020.

[32] Wiltbank N.E. and Palmer C.J., "Dynamic PRA Prospects for the Nuclear Industry," *Frontiers in Energy Research*, vol. 9, 2021, Accessed: Sep. 08, 2022. [Online]. Available: https://www.frontiersin.org/articles/10.3389/fenrg.2021.750453

[33] Siu N., "Dynamic PRA for Nuclear Power Plants: Not if but when?," Nuclear Regulatory Commission, Technical Opinion (ML19066A390), 2019.

[34] Mandelli D., Smith C., and Alfonsi A., "Integrating Classical PRA Models Into Dynamic PRA," presented at the Probabilistic Safety Assessment and Management (PSAM14), University of California, Los Angeles, 2018, p. 11.

[35] Xu A., Zhang Z., Zhang M., Wang H., Zhang H., and Chen S., "Research on Time-Dependent Failure Modeling Method of Integrating Discrete Dynamic Event Tree With Fault Tree," *Frontiers in Energy Research*, vol. 7, 2019, doi: 10.3389/fenrg.2019.00074.

[36] Apel H., Thieken A.H., Merz B., and Blöschl G., "A Probabilistic Modelling System for Assessing Flood Risks," *Nat Hazards*, vol. 38, no. 1–2, pp. 79–100, 2006, doi: 10.1007/s11069-005-8603-7.

[37] Yue S., Ouarda T.B.M.J, Bobée B., Legendre P., and Bruneau P., "The Gumbel mixed model for flood frequency analysis," *Journal of Hydrology*, vol. 226, no. 1–2, pp. 88–100, Dec. 1999, doi: 10.1016/S0022-1694(99)00168-7.

[38] Zhang L. and Singh V. P., “Bivariate Flood Frequency Analysis Using the Copula Method,” *J. Hydrol. Eng.*, vol. 11, no. 2, pp. 150–164, Mar. 2006, doi: 10.1061/(ASCE)1084-0699(2006)11:2(150).

[39] Latif S. and Mustafa F., “Bivariate Hydrologic Risk Assessment of Flood Episodes using the Notation of Failure Probability,” *Civ Eng J*, vol. 6, no. 10, pp. 2002–2023, 2020, doi: 10.28991/cej-2020-03091599.

[40] Liu Y.R., Li Y.P., Ma Y., Jia Q.M., and Su Y.Y., “Development of a Bayesian-copula-based frequency analysis method for hydrological risk assessment – The Naryn River in Central Asia,” *Journal of Hydrology*, vol. 580, p. 124349, 2020, doi: 10.1016/j.jhydrol.2019.124349.

[41] Wu Z., Shen Y., Wang H., and Wu M., “Assessing urban flood disaster risk using Bayesian network model and GIS applications,” *Geomatics, Natural Hazards and Risk*, vol. 10, no. 1, 2019, doi: 10.1080/19475705.2019.1685010.

[42] Harris R., Furlan E., Pham H.V., Torresan S., Mysiak J., and Critto A., “A Bayesian network approach for multi-sectoral flood damage assessment and multi-scenario analysis,” *Climate Risk Management*, vol. 35, 2022, doi: 10.1016/j.crm.2022.100410.

[43] Kohut P., “Evaluation of potential severe accidents during low power and shutdown operations at Surry, Unit 1: Analysis of core damage frequency from internal floods during mid-loop operations. Volume 4,” Nuclear Regulatory Commission, Technical Report NUREG/CR--6144-Vol.4, 1994. Accessed: Sep. 22, 2025. [Online]. Available: https://inis.iaea.org/records/w9zwf-sqa58

[44] Siu N., Khericha S., Conroy S., Beck S., and Blackman H., “Loss of spent fuel pool cooling PRA: Model and results,” Nuclear Regulatory Commission, Technical Report INEL--96/0334, 578718, Sep. 1996. doi: 10.2172/578718.

[45] Ebisawa K., Sugino H., and Iwabuchi Y., “Usability of Tsunami PRA based on Accidents of Fukushima Dai-Ichi NPP Under 2011 Tohoku Tsunami,” in *Proceedings of the 15th World Conference on Earthquake Engineering 2012 (15WCEE)*, Lisbon, Portugal, 2012, p. 10.

[46] Pope C. L. *et al.*, “Nuclear Power Plant Component Flooding Fragility Research,” Technical Report INL/EXT--18-45247-Rev000, 2018. doi: 10.2172/1467486.

[47] Kozlik T., “Treatment of external events in the linked event tree methodology NPP Goesgen - Daeniken example,” presented at the Probabilistic Safety Assessment (PSA) of Natural External Hazards Including Earthquakes, Prague, Czech Republic: Nuclear Energy Agency, 2014.

[48] Kaida H., Miyagawa Y., and Kihara N., “Methodology for Fragility Evaluation of a Seawall Against Tsunami Effects: Part 1 — Overflow and Physical Damage Associated With Tsunami Wave Pressure,” in *Proceedings of the 2016 24th International Conference on Nuclear Engineering*, Charlotte, North Carolina, USA: American Society of Mechanical Engineers, 2016. Accessed: Apr. 18, 2021. [Online]. Available: https://asmedigitalcollection.asme.org/ICONE/proceedings/ICONE24/50022/Charlotte,%20North%20Carolina,%20USA/252107

[49] Allsop W., Kortenhaus A., and Morris M., “Failure Mechanisms for Flood Defence Structures,” FLOODsite, T04-06–01, 2007. Accessed: Nov. 08, 2021. [Online]. Available: http://www.floodsite.net/html/partner_area/project_docs/T04_06_01_failure_mechanisms_D4_1_v1_1_p01.pdf

[50] Lee C.J. and Lee K.J., “Application of Bayesian network to the probabilistic risk assessment of nuclear waste disposal,” *Reliability Engineering & System Safety*, vol. 91, no. 5, pp. 515–532, 2006, doi: 10.1016/j.ress.2005.03.011.

[51] Segarra J.D., Bensi M., and Modarres M., “A Bayesian Network Approach for Modeling Dependent Seismic Failures in a Nuclear Power Plant Probabilistic Risk Assessment,” *Reliability Engineering & System Safety*, vol. 213, p. 107678, Sep. 2021, doi: 10.1016/j.ress.2021.107678.

[52] Tolo S., Patelli E., and Beer M., “Robust vulnerability analysis of nuclear facilities subject to external hazards,” *Stoch Environ Res Risk Assess*, vol. 31, no. 10, pp. 2733–2756, 2017, doi: 10.1007/s00477-016-1360-1.

[53] García-Herrero S., Mariscal M. A., Gutiérrez J. M., and Toca-Otero A., “Bayesian network analysis of safety culture and organizational culture in a nuclear power plant,” *Safety Science*, vol. 53, pp. 82–95, Mar. 2013, doi: 10.1016/j.ssci.2012.09.004.

[54] Groth K., Wang C., and Ali Mosleh, “Hybrid causal methodology and software platform for probabilistic risk assessment and safety monitoring of socio-technical systems,” *Reliability Engineering & System Safety*, vol. 95, no. 12, pp. 1276–1285, Dec. 2010, doi: 10.1016/j.ress.2010.06.005.

[55] Wang C., “Hybrid Causal Logic Methodology for Risk Assessment,” Dissertation, University of Maryland, College Park, 2007.

[56] Mosleh A., Groth K., and Zhu D., “A PRA Software Platform for Hybrid Causal Logic Risk Models,” presented at the 9th International Conference on Probabilistic Safety Assessment and Management (PSAM9), Hong Kong, 2008. Accessed: Sep. 22, 2025. [Online]. Available: https://www.researchgate.net/publication/255171881_A_PRA_Software_Platform_for_Hybrid_Causal_Logic_Risk_Models

[57] Zwirglmaier K. and Straub D., “A discretization procedure for rare events in Bayesian networks,” *Reliability Engineering & System Safety*, vol. 153, pp. 96–109, 2016, doi: 10.1016/j.ress.2016.04.008.

[58] Salmerón A., Rumí R., Langseth H., Nielsen T.D., and Madsen A.L., “A Review of Inference Algorithms for Hybrid Bayesian Networks,” *Journal of Artificial Intelligence Research*, vol. 62, pp. 799–828, Aug. 2018, doi: 10.1613/jair.1.11228.

[59] Langseth H., Nielsen T.D., Rumí R., and Salmerón A., “Inference in hybrid Bayesian networks,” *Reliability Engineering & System Safety*, vol. 94, no. 10, pp. 1499–1509, Oct. 2009, doi: 10.1016/j.ress.2009.02.027.

[60] Modarres M. and Groth K., *Reliability and Risk Analysis*, 2nd ed. in What Every Engineer Should Know. 2023.

[61] Bensi M., “A Bayesian Network Methodology for Infrastructure Seismic Risk Assessment and Decision Support,” Dissertation, University of California, Berkely, Berkely, CA, 2010. Accessed: Aug. 18, 2021. [Online]. Available: https://digitalassets.lib.berkeley.edu/etd/ucb/text/Bensi_berkeley_0028E_10906.pdf

[62] Ding J., “Probabilistic Inferences in Bayesian Networks,” *arXiv.org*, Nov. 2010, doi: 10.5772/46968.

[63] Segarra J.D., “A Bayesian Network Perspective on the Elements of a Nuclear Power plant Multi-Unit Seismic Probabilistic Risk Assessment,” University of Maryland, College Park, 2021.

[64] Mohammadi S. *et al.*, “Bayesian-Motivated Probabilistic Model of Hurricane-Induced Multimechanism Flood Hazards,” *J. Waterway, Port, Coastal, Ocean Eng.*, vol. 149, no. 4, p. 04023007, Jul. 2023, doi: 10.1061/JWPED5.WWENG-1921.

[65] “The 100-Year Flood | U.S. Geological Survey.” Accessed: Sep. 22, 2025. [Online]. Available: https://www.usgs.gov/water-science-school/science/100-year-flood

[66] Prasad R. and Meyer P., “Technical Basis for Probabilistic Flood Hazard Assessment (PFHA) for Riverine Flooding,” presented at the Second Annual PFHA Workshop, U.S. NRC Headquarters, Jan. 23, 2017.

[67] Kanney J., Nadal-Caraballo, N.C., and Gonzalez V.M., “Coastal Flooding PFHA Pilot Study,” presented at the 5th Annual PFHA Research Workshop, U.S. NRC Headquarters, Feb. 2020.

[68] Kasmalkar I. *et al.*, “Flow-tub model: A modified bathtub flood model with hydraulic connectivity and path-based attenuation,” *MethodsX*, vol. 12, p. 102524, 2023, doi: 10.1016/j.mex.2023.102524.

[69] Ma Z., Zhang S., Pope C. L., and Smith C., “Research to Develop Flood Barrier Testing Strategies for Nuclear Power Plants,” Nuclear Regulatory Commission, Technical Report NUREG/CR-7279 INL/EXT-19-56427, 2021.

[70] Kennedy R.P. and M.K. Ravindra, “Seismic fragilities for nuclear power plant risk studies,” *Nuclear Engineering and Design*, vol. 79, no. 1, pp. 47–68, May 1984, doi: 10.1016/0029-5493(84)90188-2.

[71] Alfonsi A., Rabiti C., Mandelli D., Cogliati J.J., Kinoshita R.A., and Naviglio A., “RAVEN and Dynamic Probabilistic Risk Assessment: Software Overview,” Idaho National Lab, Technical Report INL/CON-14-31785, 2014.

[72] “Neutrino Dynamics.” Accessed: Feb. 02, 2024. [Online]. Available: http://www.neutrinodynamics.com/

[73] “CHS - Study,” U.S. Army Corps of Engineers. Accessed: Apr. 06, 2022. [Online]. Available: https://chs.erdc.dren.mil/Study

[74] Baker J., Bradley B., and Stafford P., *Seismic Hazard and Risk Analysis*. Cambridge: Cambridge University Press, 2021. doi: 10.1017/9781108425056.

[75] Dasgupta B., “Evaluation of Methods used to Calculate Seismic Fragility Curves,” Center for Nuclear Waste Regulatory Analyses, San Antonio, Texas, ML17122A268, 2017. Accessed: Apr. 25, 2021. [Online]. Available: https://www.nrc.gov/docs/ML1712/ML17122A268.pdf

[76] Kennedy R.P., Murray R.C., Ravindra M.K., Reed J.W., and Stevenson J.D., “Assessment of seismic margin calculation methods,” Nuclear Regulatory Commission, Technical Report NUREG/CR-5270, UCID-21572, 1989. doi: 10.2172/6428052.

[77] American Society of Civil Engineers, Structural Engineering Institute, Structural Engineering Institute, and Structural Engineering Institute, Eds., *American Society of Civil Engineers seismic design criteria for structures, systems, and components in nuclear facilities*. in ASCE standard. Reston, Va: American Society of Civil Engineers, 2005.

[78] “Pipe Penetration Seals.” PROCO, 9/13. [Online]. Available: https://www.procoproducts.com/product/proco-pen-seal/

[79] “Seal Pipe Penetrations.” Innerlynx. [Online]. Available: https://apsonline.com/innerlynx-wall-sleeves/

[80] “Wall Sleeves.” Link-Seal. [Online]. Available: https://www.ejprescott.com/hubfs/media/reference/WallSleevesA-44.pdf

[81] “Watertight sealing for pipes through concrete walls.” Westatantic Tech Corp. [Online]. Available: https://westatlantictech.com/link-chain-seals

[82] Katrina Groth, Zhu, and Ali Mosleh, “Hybrid methodology and software platform for probabilistic risk assessment,” in *2008 Annual Reliability and Maintainability Symposium*, Las Vegas, NV, USA: IEEE, 2008, pp. 411–416. doi: 10.1109/RAMS.2008.4925831.

[83] I. A. E. Agency, “Seismic Hazards in Site Evaluation for Nuclear Installations,” International Atomic Energy Agency, Text, 2022. Accessed: Sep. 07, 2025. [Online]. Available: https://www.iaea.org/publications/14665/seismic-hazards-in-site-evaluation-for-nuclear-installations

[84] Mosleh A., Groth K., Wang C., and Zhu D., “Methodology and Software Platform for Multi-Layer Causal Modeling,” 2008.

[85] “GeNIe Modeler – BayesFusion.” Accessed: Nov. 15, 2023. [Online]. Available: https://www.bayesfusion.com/genie/

[86] “SAPHIRE | Home.” Accessed: Jul. 25, 2025. [Online]. Available: https://saphire.inl.gov/#/

[87] Z. Ma, T. Wierman, and K. J. Kvarfordt, “Industry-Average Performance for Components and Initiating Events at U.S. Commercial Nuclear Power Plants: 2020 Update,” INL, INL/EXT-21-65055, Nov. 2021. Accessed: Jul. 17, 2024. [Online]. Available: https://nrcoe.inl.gov/ccf_pe/

[88] Zhegang Ma, “Enhanced Component Performance Study: Emergency Diesel Generators 1998-2020,” Idaho National Laboratory, Technical Report INL/RPT-22-66601-Rev.0, Mar. 2022. doi: 10.2172/1894882.

[89] Zhang S., Atwood C., and Zhegang Ma, “Developing Component-Specific Prior Distributions for Common Cause Failure Alpha Factors,” Idaho National Lab, Technical Report INL/EXT--21-65527-Rev.001, 2341474, Jan. 2023. doi: 10.2172/2341474.

[90] Bobbio A., Portinale L., Minichino M., and Ciancamerla E., “Improving the analysis of dependable systems by mapping fault trees into Bayesian networks,” *Reliability Engineering & System Safety*, vol. 71, no. 3, pp. 249–260, Mar. 2001, doi: 10.1016/S0951-8320(00)00077-6.

[91] Liu Z., Carr M.L., Nadal-Caraballo, N.C., Aucoin L.A., Yawn M.C., and Bensi M., “A Multi-Tiered Bayesian Network Coastal Compound Flood Analysis Framework,” *Coastal Engineering*, vol. 204, 2025, doi: 10.1016/j.coastaleng.2025.104895.

[92] Gibson E.M. and Bensi M., “Proposed Bayesian Network Framework to Model Multisite Seismic Hazard with Existing Probabilistic Seismic Hazard Analysis Results,” *ASCE-ASME Journal of Risk and Uncertainty in Engineering Systems, Part A: Civil Engineering*, vol. 10, no. 3, p. 04024049, Sep. 2024, doi: 10.1061/AJRUA6.RUENG-1252.